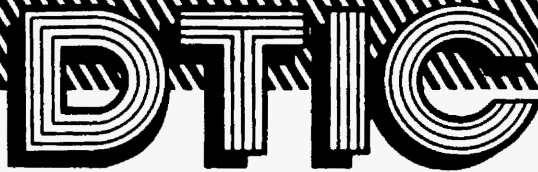


UNCLASSIFIED/UNLIMITED

410194

The logo for the Defense Technical Information Center (DTIC) is displayed in a large, stylized, outlined font. The letters 'D', 'T', and 'I' are connected, and the 'C' is a large circle. The background behind the logo is a black and white diagonal hatched pattern.

**NOTICE**  
This document has been withdrawn from the DDC bulk storage. It is the responsibility of the recipient to promptly mark it to indicate the reclassification notice shown herein.

# Technical Report

distributed by



**Defense Technical Information Center  
DEFENSE LOGISTICS AGENCY**

Cameron Station • Alexandria, Virginia 22314

UNCLASSIFIED/UNLIMITED

**UNCLASSIFIED**

**UNCLASSIFIED**

TECHNICAL LIBRARY

①

Copy No. 153 A

Document No. \_\_\_\_\_

Copy No. \_\_\_\_\_

*ation*

**ASTLE**

\_\_\_\_\_

STIA  
MAY 20 1953

Report for Project 4.1

PHYSICAL FACTORS AND DOSIMETRY IN THE MARSHALL ISLAND RADIATION EXPOSURES

**338 337**

RESTRICTED

**RESTRICTED DATA**

This document contains restricted data as defined in the Atomic Energy Act of 1954. Its transmittal or the disclosure of its contents in any manner to an unauthorized person is prohibited.

HEADQUARTERS FIELD COMMAND, ARMED FORCES SPECIAL WEAPONS PROJECT  
SANDIA BASE, ALBUQUERQUE, NEW MEXICO

**UNCLASSIFIED**

**SECRET**

UNCLASSIFIED

AD 338337

CLASSIFICATION CHANGED  
TO: UNCLASSIFIED  
FROM: CONFIDENTIAL  
AUTHORITY: DNA

116 12 Dec 80



UNCLASSIFIED

**UNCLASSIFIED**

Reproduced directly from manuscript copy by  
AEC Technical Information Service Extension  
Oak Ridge, Tennessee

Comments relative to this report may be made to

Chief, Army Forces Special Weapons Project  
Washington, D. C.

If this report is no longer needed, return to  
AEC Technical Information Service Extension  
P. O. Box 401  
Oak Ridge, Tennessee

**UNCLASSIFIED**

REG. NO. 18853 ✓

LOG. NO. 9798

WDSB

**UNCLASSIFIED**

Operation CASTLE

① Addendum Report for Project 4.1.

① PHYSICAL FACTORS AND DOSIMETRY IN THE MARSHALL ISLAND  
RADIATION EXPOSURES [10]

\*This document contains information affecting the National  
Defense of the United States within the meaning of the National  
Espionage Laws, Title 18, U. S. C., Section 793 and  
in any manner to an unauthorized person is prohibited  
by law.

by  
C. A. Sondhaus  
V. P. Bond

① Location 455, ② 12/16/55, ③ 11A

**RESTRICTED DATA**

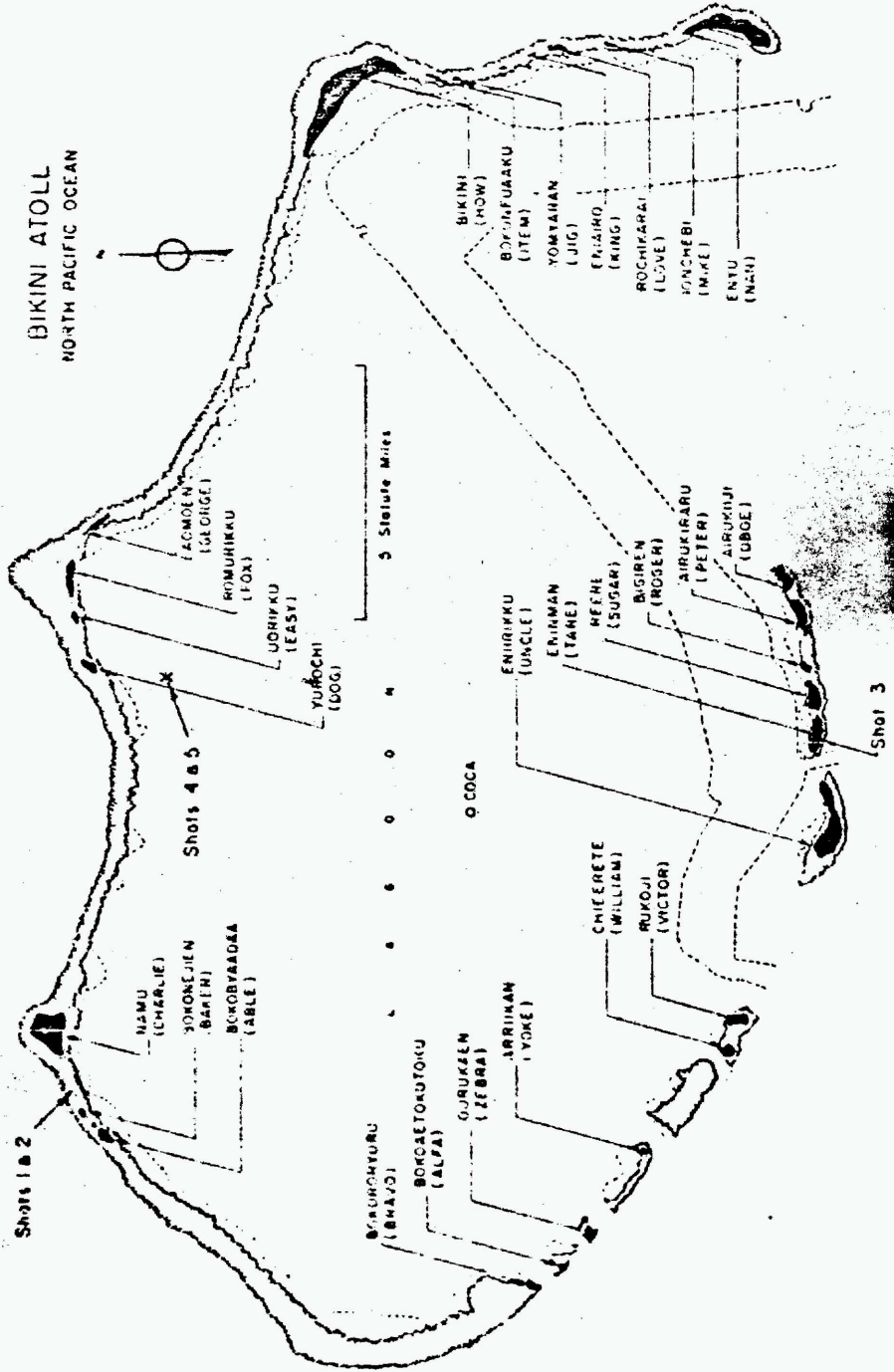
This document contains restricted data as defined in the Atomic Energy Act of 1954. Its transmittal or the disclosure of its contents in any manner to an unauthorized person is prohibited.

U. S. Naval Radiological Defense Laboratory  
San Francisco 24, California

**UNCLASSIFIED**



BIKINI ATOLL  
NORTH PACIFIC OCEAN



UNCLASSIFIED

GENERAL SHOT INFORMATION

	Shot 1	Shot 2	Shot 3	Shot 4	Shot 5	Shot 6
DATE	1 March	27 March	7 April	26 April	5 May	14 May
CODE NAME (Unclassified)	Bravo	Romeo	Koon	Union	Yankee	Nectar
TIME*	06:40	06:25	06:15	06:05	06:05	06:15
LOCATION	Bikini, West of Charlie (Namu) on Reef	Bikini, Shot 1 Crater	Bikini, Tore (Eninman)	Bikini, on Barge at Intersection of Arcs with Radii of 6900 from Dog (Yurachi) and 3 Statute Miles from Fox (Aomoe)	Bikini, on Barge at Intersection of Arcs with Radii of 6900 from Dog (Yurachi) and 3 Statute Miles from Fox (Aomoe)	Eniwetok, IVY Mike Crater, Fiora (Elugelab)
TYPE	Land	Barge	Land	Barge	Barge	Barge
HOLMES & NARVER COORDINATES	N 170,617.17 E 76,163.98	N 170,635.05 E 75,950.46	N 100,154.50 E 109,799.00	N 161,698.83 E 116,800.27	N 161,424.43 E 116,688.15	N 147,750.00 E 67,790.00

\* APPROXIMATE

UNCLASSIFIED

## ABSTRACT

This report is an addendum to the final report of Project 4.1, Operation CASTLE. Its purpose is to consider the physical factors and dosimetry of the fallout on the Marshall Islands from the first shot of Operation CASTLE.

Data was summarized from field Radiological Safety surveys, fallout radiochemical studies, and fallout gamma spectral measurements. The influence of these and other factors on an evaluation of survey meter response and total dose estimates was considered. Estimates of fallout duration times and energy distribution of the dose from a plane source were made and the effect of diffuse source-geometry on the depth-dose to air-dose relationship was considered. Superficial doses from soft gamma and beta radiation were also considered.

Since the fallout incident created an initial emergency during which data collection was of secondary importance, attempts to reconstruct the event have been uncertain. Much of the data was indicative rather than exact. However, a fairly consistent estimate of external gamma dosage was possible, although the question of beta exposure remains mostly unanswered. It has been assumed that no significant neutron or alpha particle exposure occurred. Internal doses from inhaled or ingested material and the bio-medical aspects of the incident have been discussed in other CASTLE Project 4.1 reports.

It was concluded that: (1) the AN/PDR-39A requires a correction factor of about plus 20 percent in dose-rate readings made under the conditions described; (2) decay of the radioactivity of the fallout is believed expressible by the factor of  $T^{-0.83}$ ; (3) the external gamma dose was delivered primarily by radiation energies of 100, 700, and 1500 kev; (4) the beta dose was delivered by beta radiation of maximum energies of 0.3 and 1.8 Mev, mostly from fallout deposited on the skin itself; (5) the exposures occurred between 4 and 78 hours after the detonation - the fallouts were probably of 12-hours duration; (6) diffuse source geometry increased the midline dose by about 50 percent compared to the midline dose which would have resulted from a bilateral narrow beam exposure of the same air-dose; (7) error in the estimates is believed to be less than 50 percent; and (8) total air gamma doses were estimated as follows: Rongerik, 86 r; Rongelap, 182 r; Ailinginae, 81 r; and Utirik, 13 r.

## FOREWORD

This report is one of the reports presenting the results of the 34 projects participating in the Military Effects Program of Operation CASTLE. For readers interested in other pertinent test information, reference is made to WT-934, Report of the Commander, Task Unit 13, Military Effects Program. This summary report includes the following information of possible general interest.

- (a) An over-all description of each detonation, including yield, height of burst, ground zero location, time of detonation, ambient atmospheric conditions at detonation time, etc., for the operation.
- (b) Discussion of all project results.
- (c) A summary of each project, including objectives and results.
- (d) A complete listing of all reports covering the Military Effects Test Program.

## ACKNOWLEDGMENTS

The encouragement and assistance of Dr. E. P. Cronkite, Project Officer of Project 4.1, Operation CASTLE, is gratefully acknowledged. LTJG R. Sharp (MSC) USN aided in the collection of much of the information in the field and assisted with the calculations.

Data relevant to dosage calculation were made available by many sources. Information on energy distribution of the gamma radiation was furnished by Dr. C. S. Cook and the Nuclear Radiation Branch at the U. S. Naval Radiological Defense Laboratory (NRDL). Radiochemical data supporting calculated radioactive decay rates were supplied by Dr. C. F. Miller, Dr. N. E. Ballou, and the Chemical Technology Division of NRDL, and Dr. H. W. Spence of the Los Alamos Scientific Laboratory (LASL).

CDR F. L. Chambers (MSC) USN of the Naval Medical Research Institute (NMRI) kindly furnished field depth dose data obtained at Operation UFSHDT/MOCHOLE. Particular thanks is due: Colonel C. E. Maupin (MC) USA of Field Command, Armed Forces Special Weapons Project, and Dr. H. Scoville, of Headquarters, Armed Forces Special Weapons Project.

## CONTENTS

ABSTRACT . . . . .	5
FOREWORD . . . . .	6
ACKNOWLEDGMENTS . . . . .	6
ILLUSTRATIONS . . . . .	8
TABLES . . . . .	8
CHAPTER 1 INTRODUCTION . . . . .	9
CHAPTER 2 FIELD DOSAGE DATA . . . . .	10
2.1 Early Data . . . . .	10
2.2 Exposure Conditions . . . . .	10
2.3 Later Surveys . . . . .	12
CHAPTER 3 FALLOUT CHARACTERISTICS . . . . .	14
3.1 Experimental Data . . . . .	14
3.2 Calculated Decay Rates . . . . .	14
CHAPTER 4 GAMMA ENERGY-DOSE SPECTRUM . . . . .	17
4.1 Photon Flux Spectrum . . . . .	17
4.2 Dose-Energy Distributions for Plane Source Geometry . . . . .	18
4.3 Beta Energy . . . . .	21
CHAPTER 5 METER RESPONSE FACTORS . . . . .	25
5.1 Energy Response . . . . .	25
5.2 Geometry Response . . . . .	27
CHAPTER 6 DURATION AND TIME DISTRIBUTION OF DOSES . . . . .	30
6.1 Available Data . . . . .	30
6.2 Estimates of Fallout Duration . . . . .	31

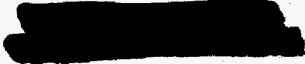
CHAPTER 7 EXPOSURE GEOMETRY EFFECTS. . . . .	34
7.1 Discussion. . . . .	34
7.2 Experimental Simulation and Geometry Factor . . . . .	35
CHAPTER 8 TOTAL DOSE ESTIMATES . . . . .	38
8.1 Calculated Values . . . . .	38
8.2 Discussion. . . . .	38
8.3 Soft Gamma and Beta Components. . . . .	39
CHAPTER 9 CONCLUSIONS. . . . .	43
REFERENCES. . . . .	44

### ILLUSTRATIONS

3.1 Calculated Total Activity Versus Time. . . . .	16
4.1 Dose-Energy Distribution, Shot 4, H + 5.3 Day Sample. . . . .	22
4.2 Dose-Energy Distribution, Shot 1, H + 4.1 Day Sample. . . . .	23
4.3 Dose-Energy Distribution, Shot 1, H + 5.2 Day Sample. . . . .	24
5.1 Energy Response of Survey Meter AN/PDR-TLB . . . . .	26
5.2 Directional Response of Survey Meter AN/PDR-TLB. . . . .	29
6.1 Fallout Dose Rate Versus Time Estimates, Rongerik Atoll . . . . .	33
7.1 Depth-Dose Curves, 36-cm Phantom, 1.2 Mev. . . . .	36
7.2 Depth-Dose Curves, 36-cm Phantom, 200 KVP. . . . .	37
8.1 Cumulative Air-Dose with Time, Rongelap Atoll. . . . .	40
8.2 Field Depth-Dose Measurement, Operation UFSHOT-KNOTHOLE. . . . .	41

### TABLES

2.1 Radiation Intensity at Rongerik During Early Fallout (Shot 1) . . . . .	11
2.2 Early Dose Rate Data (2 to 3 March). . . . .	11
2.3 Film Badge Readings on Rongerik. . . . .	12
2.4 Later Dose Rate Data (8 to 11 March) . . . . .	13
4.1 Shot 4, H + 9 1/2 Hr. . . . .	18
4.2 Shot 4, H + 5.3 Days . . . . .	20
4.3 Shot 1, H + 4.1 Days . . . . .	20
4.4 Shot 1, H + 5.2 Days . . . . .	21
5.1 Total Energy Response Factors for AN/PDR-39A . . . . .	27
6.1 Fallout and Evacuation Times . . . . .	31
8.1 Total Gamma Doses. . . . .	39



CHAPTER 1

INTRODUCTION

The fallout on the Marshall Island atolls of Rongelap, Rongerik, Ailinginae, and Utirik from the first shot of the series beginning 1 March 1954 created an initial emergency during which the gathering of data was of secondary importance. This fundamental fact has resulted in uncertainty in all attempts to reconstruct the circumstances of the event. Calculation of the external doses received by the exposed individuals has required that available information be supplemented by assumptions. Much of the information itself was necessarily more indicative than exact. In spite of these difficulties, the cooperation of many individuals and groups made it possible to develop a fairly consistent estimate of external gamma dosage, although the question of beta exposure must remain mostly unanswered.

It has been assumed that no significant neutron or alpha particle exposure occurred. Thus, the main consideration in this report is the total body gamma radiation exposure. Internal doses from inhaled or ingested material have been discussed elsewhere (Reference 1).

Data which form the basis of the analysis were furnished by several sources which are listed in the References. These represent measurements made both in the field and in the laboratory in the period immediately following the exposure. Later information has also been included wherever it was available. A summary of these results appears in Reference 16, which covers the biological and medical aspects of the incident.

## CHAPTER 2

### FIELD DOSAGE DATA

#### 2.1 EARLY DATA

When the exposures began, no monitoring personnel were in the vicinity of any of the contaminated islands. One of the first indications of a fallout was visual, when a snow-like material was observed in the air on each of the islands. The reports on the times of observation, although conflicting, serve to establish the time of arrival of the cloud at each island, except at Rongerik (see Chapter 6). Here the first evidence of a radiation field was observed when a low-level gamma background monitoring instrument at the weather station began to register and then went off scale at 100 mr/hr at approximately H + 7.4 hours. Table 2.1 lists the readings of this instrument during the half hour preceding this time (Reference 2). These data are the only information available on the initial rate of increase of gamma dose rate on any of the islands.

At the time of evacuation of the military personnel from Rongerik on 2 March and the Marshallese from Rongelap, Ailinginae, and Utirik on 3 March, dose rate readings were made on each island. This was done with AN/PDR-39 radiation survey meters which were available at the time and which had not been calibrated beforehand. Their operating condition was not known at the time of use. The readings of these instruments are given in Table 2.2, and constitute the earliest data on gamma dose rates in any of the areas (Reference 3).

#### 2.2 EXPOSURE CONDITIONS

So far as is known, the individuals exposed on Rongelap and Ailinginae remained outdoors and had no access to shelter of any kind on the islands. No measures were intentionally taken to protect the skin, but clothing was worn to a degree sufficient to shield from most of the deposited beta activity. In addition, much of the fallout skin contamination was removed from some individuals, as a result of their swimming and fishing in the lagoon at the time. On the other hand, the heavy coconut oil hair dressing used by the Marshallese tended to concentrate radioactivity in the hair. The surface contamination on the ground was apparently fairly uniform over the islands, so that the calculation of average gamma doses from this source appears justified.

TABLE 2.1 - Radiation Intensity at Rongerik  
During Early Fallout (Shot 1)

Time after H hour (hr)	Gamma Dose Rate (mr/hr, background)
6.5 (1345 1 March)	0.03
6.87	0.18
6.91	0.70
6.95	2.7
7.04	3.6
7.12	10.5
7.20	30
7.29	60
7.37	100

TABLE 2.2 - Early Dose Rate Data (2 to 3 March)

Island	Time after H hour (hr)	Average Dose Rate (mr/hr)
Rongelap	H + 36	1500
Rongerik	H + 28.5	2000
Ailinginae	H + 58	445
Utirik	H + 55	160

On Rongerik, the exposed individuals recognized the nature of the fallout, put on protective clothing, and took advantage of the partial gamma shielding afforded by Butler-type buildings in the area, staying indoors as far as possible. The radiation dose rate encountered by an individual on this island thus depended on his whereabouts and probably varied by a factor of two between maximum and minimum values in different areas at a given time. The estimation of dose received by any one individual of the Rongerik group was thus subject to considerable uncertainty, since no complete record of movements was kept.

However, a group of film badge readings was obtained covering a range of values which varied with exposure conditions (Reference 3). These readings are summarized in Table 2.3. Several badges were worn both outdoors and indoors. One badge which remained outdoors over the 28.5-hour exposure reached the upper limit of 98 r given in the table. Several other badges kept inside a refrigerator indoors gave the lowest value of 38 r. Skin contamination in the Kongerik group appeared to have been much reduced by the protective measures taken and the resulting beta doses appeared clinically to have been clearly lower than in the other groups.

TABLE 2.3 - Film Badge Readings on Kongerik

Location of Badges	Calculated Dose to Badges (r)
Indoors and Out	44 to 52
Outdoors only	98
Inside Refrigerator Indoors	38

### 2.3 LATER SURVEYS

During the period 8 to 11 March, more extended surveys of each of the islands were made by a monitoring team equipped with five AN/PDR-39 instruments (Reference 4). Twenty-four hours previous to the departure of the survey party, three of the instruments were calibrated on an 80-curie  $\text{Co}^{60}$  source and cross checked at 0.320 r/hr, where they were found to be in close agreement. Using these instruments, measurements were made in the inhabited areas of all four islands at waist height (approximately 3 feet above ground). Table 2.4 is a summary of these data. Since these later readings were made under better controlled conditions than the emergency surveys at the times of evacuation given in Table 2.2, the data of Table 2.4 were taken to be the best measurement at a given time of the gamma dose rates in air and were used in the calculation of the total external gamma dose.

No information existed on the quantity of beta contamination on the skin of any of the exposed individuals. Further, no experimental data allowed any reliable calculation of the beta dose rate to an individual from fission products on the ground. Thus the only basis for any estimate of external beta dosage was data from other field tests and fallout measurements. This question is discussed further in Chapter 6, and a rough estimate for possible beta dose from the ground is made there.

TABLE 2.4 - Later Dose Rate Data (8 to 11 March)

Location	Time after H hour (days)	Avg. Dose Rate ( $\mu$ r/hr)
Rongelap:		
average	H + 7	375
maximum		450
one point in village	H + 7	280
	H + 10	170
Rongerik:		
*average outdoors	H + 9	280
*maximum outdoors		300
Ailinginae:		
average	H + 9	100
Utirik:		
average	H + 8	40

\*Dose rate inside structures found to be about  $\frac{1}{2}$  that outside.

## CHAPTER 3

### FALLOUT CHARACTERISTICS

#### 3.1 EXPERIMENTAL DATA

In order to calculate a total gamma dose received by an individual in an area where dose rate was measured at a given time, a value for the rate of change of radiation intensity during the exposure period must be assumed. The latter quantity has often been approximated using the well known way-Wigner ( $t^{-1.2}$ ) decay law. In this case however, it was known that large amounts of  $\text{Np}^{239}$  and  $\text{Np}^{240}$  were to be expected in the fallout of the 1 March shot, making its early decay characteristics as well as its energy spectrum somewhat different from those of previous detonations. It was therefore decided, that the value of decay rate assumed to exist during the exposures should be based, as far as possible, upon experimental data from this test.

Unfortunately, no decay rates were followed closely in any of the immediate areas where the exposures occurred, and it is known that the radiochemical composition and decay rate of the fission product mixture usually vary both with place and time. However, early decay rates in the Bikini lagoon itself had been measured in a series of fallout samples taken at other points nearer the site of the detonation (Reference 5). Since these values were the best data available, they were used in the calculations and were assumed to hold for the fallout on each of the islands.

The early samples showed a consistent pattern among various locations and a decay exponent ( $n$ ) of between 0.8 and 0.9 in Equation 3.1.

$$A = A_1(t/t_1)^{-n} \quad (3.1)$$

where:  $A$  = activity (d/m) at time  $t$ .

This decay exponent ( $n$ ) was found experimentally to fit the data for the period  $H + 5$  to  $H + 50$  hours. The observed values are given in Reference 5.

#### 3.2 CALCULATED DECAY RATES

These decay rates were compared with calculated values based on the presence of  $\text{Np}^{239}$  and  $\text{Np}^{240}$  in the fallout mixture. The calculations were made on the assumption that the relative abundance of  $\text{Np}^{239}$

at 4 hours after detonation was 1.3 d/m per  $10^4$  fissions and that of  $U^{240}$  was 2.7 d/m per  $10^4$  fissions while the gross fission product decay followed the Hinter-Rallou exponents and its activity at 4 hours was 13 d/m per  $10^4$  fissions (Reference 6). This value of  $Np^{239}$  activity follows from a calculated neutron capture-to-fission ratio of 0.78 in the  $U^{238}$  tamper.

Using the half-life of 2.33 days for  $Np^{239}$  and 14 for  $U^{240}$  and combining these data with those for the total rate of decay of the fission products as assumed above, a total activity curve was calculated. This is illustrated in Figure 3.1. It is seen that a decay rate exponent of 0.83 between  $H + 4$  and  $H + 23$  hours; of 1.1 between  $H + 23$  and  $H + 120$  hours; and 1.6 from  $H + 5$  to about  $H + 14$  days fits these portions of the curve. The presence of the measured decay rates thus agreed with other parameters of the detonation during the exposure and survey periods. Figure 3.1 was used in the dosage calculations. The effect on dosage of the energy spectrum resulting from this composition is discussed in Chapter 4.

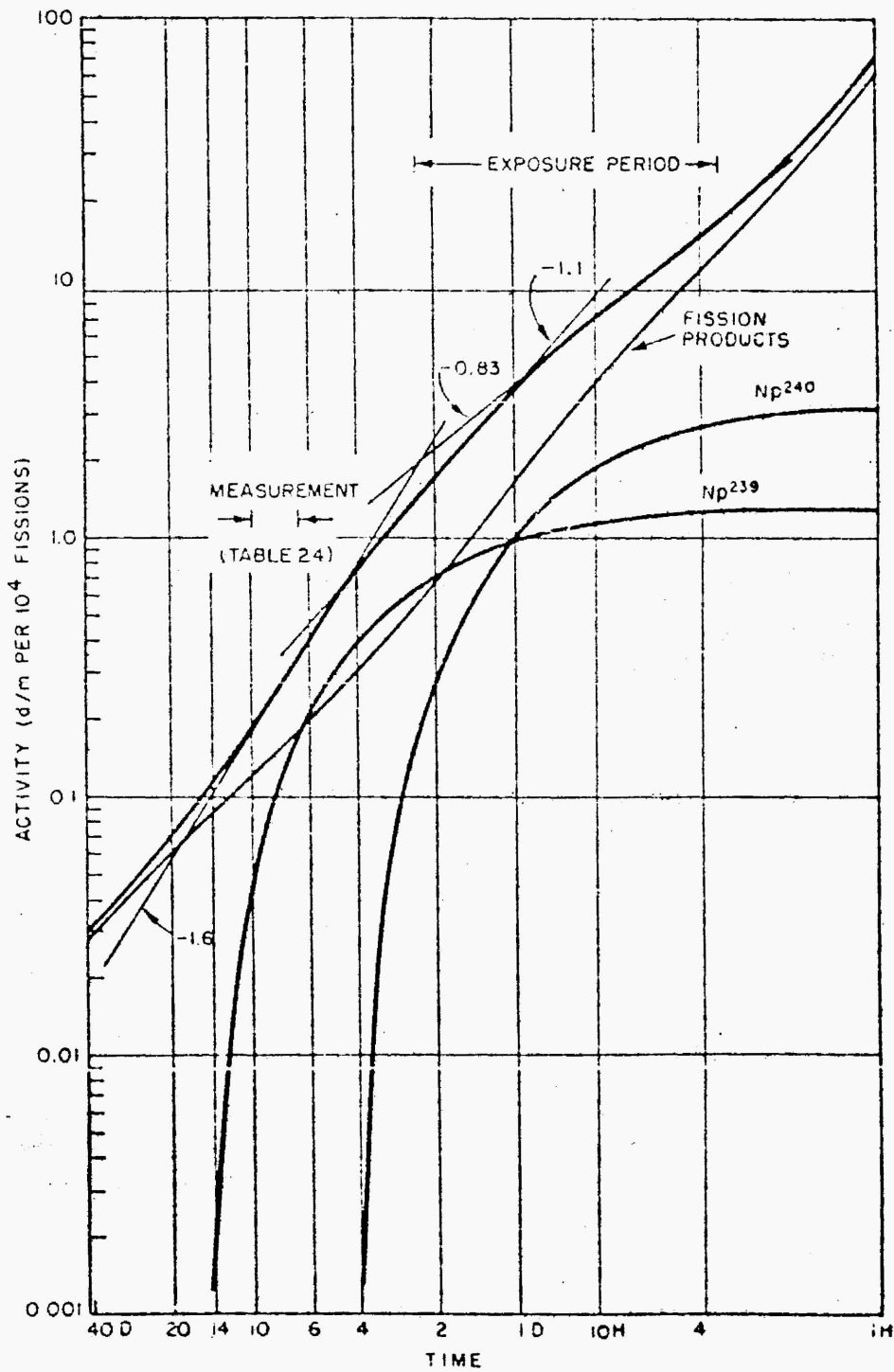


Fig. 3.1 Calculated Total Activity Versus Time

## CHAPTER 4

### GAMMA ENERGY-DOSE SPECTRUM

#### 4.1 PHOTON FLUX SPECTRUM

The fallout material deposited on the ground produced a large area plane source of radiation. Before a total gamma dose could be calculated, it was necessary to correct the dose rate readings in air taken with the survey instruments with the meter response factors found to be necessary for different energy regions. Further, to estimate the distribution of dose with depth in tissue required a knowledge of energy distribution of the incoming flux in a given exposure geometry.

For a source as large as these fallout fields, this energy distribution will be a function both of the original source energy and the energy degradation effect of passage through intervening air. A method of evaluating the latter, which was due mainly to Compton scattering in air for the fission product energy region, has been presented in Reference 7. This technique was employed here. Energy spectra of the CASTLE fallout itself has been measured with a scintillation spectrometer on a series of cloud samples as early as H + 4 days. The data have been published in Reference 8. The preliminary data on the earliest of these, a 94-hour-old cloud sample, were used in the calculations summarized in Reference 16. These are given in Table 4.1 (Reference 9). This 94-hour sample from Shot 1 represents the closest approach to the actual time during which the exposures occurred.

After the conclusion of the test series, analysis of early data from other shots continued and later spectra for all shots were analyzed. None of the other spectra are for times as early as H + 94 hours. For the later detonations the proportion of  $\text{Np}^{239}$  (average gamma energies  $E_1 = 243$  kev, 40 percent;  $E_2 = 105$  kev, 11 percent;  $E_3 = 58$  kev, 49 percent) in the fallout samples was found to be much higher than that given in Table 4.1. An extreme case, for example, is the data for Shot 4 on 26 April at H + 5.3 days which is given in Table 4.2. Here the low energy portion of less than 100 kev was measured as 60 percent of the total photon flux. Two later determinations on another Shot 1 sample (1-L, Table 3 of Reference 8) show these low energy proportions as 55 percent at H + 4.1 days and 54 percent at H + 5.2 days as well (Tables 4.3 and 4.4). Later data thus tended to show that the initial estimate of low energy radiation was low. Hence, revised estimates of the total doses will be presented here on the basis of the additional data for which the counting statistics were better than on the Shot 1, H + 94 hour sample. These spectra, it must be emphasized, are for

samples taken soon after the detonation in the cloud itself at some distance from the atolls (Reference 5). Again they represent the best data available and, in the absence of contrary evidence, had to be taken as typical of the fallout on the islands.

TABLE 4.1 - Shot 1, H + 94 Hr

Energy (Mev)	Percent of Flux	Cumulative Percent Dose (See Text)
1.59	7.04	100
1.37	0.99	83
1.27	0.80	
0.96	2.70	80
0.84	3.71	66
0.76	15.11	
0.66	19.24	36
0.50	12.15	21
0.27	4.82	
0.22	6.00	12
0.10	20.24	
0.068	5.04	8
0.018	2.17	

#### 4.2 DOSE-ENERGY DISTRIBUTIONS FOR PLANE SOURCE GEOMETRY

To compute the proportion of total air-dose due to a given energy interval in the degraded spectrum which resulted from the spectrum of the original sample, the dose from the spectrum due to the emitter distributed as an infinite plane source was calculated by summing the contributions over all path lengths in air. By dividing the original H + 94 hour spectrum into 13 energy regions and carrying out this process (Reference 7) for each, a cumulative dose versus energy curve resulted. The cumulative doses are given in Tables 4.1, 4.2, and 4.3. From these curves, a differential histogram of percent dose versus energy interval was determined which represents the percent of dose

delivered to the surface of the exposed individual at a height of 3 feet above the plane by photons with energies in each of these intervals (Figures 4.1, 4.2, and 4.3).

The process consists essentially of the following steps:

1. For each source energy, calculating the dose per photon contributed by the unscattered portion of the radiation from each increment of source area. This requires an expression involving "true" and total absorption coefficients in air, exponential integral, source energy, and fraction of dose due to unscattered photons of that energy.
2. For each source energy, calculating a weighting factor (or relative dose) by multiplying the dose per photon in Step 1, above, by the number of source photons with that energy.
3. For each source energy, estimating the fraction of dose due to source photons originally of that energy but degraded by scattering to energies less than each of a set of arbitrarily chosen energy values.
4. Computing the total dose due to all photons with energies up to each chosen energy value by summing the product of Steps 2 and 3, above, for each of the original source energies.

The result is an integral or cumulative air-dose spectrum; i.e., a plot of photon energy versus the air-dose resulting from all photons from zero to that energy. From this, a rough differential dose histogram is obtained by subtracting ordinates on the integral curve at the endpoints of each chosen energy interval. The use of graphical and numerical methods makes the technique quite applicable to the determination of a number of such dose-energy distributions.

Figure 4.2 of Reference 16 depicts the differential air-dose distribution for the Shot 1 H + 94 hour data, in percent of dose per 0.05 Mev interval versus energy in Mev. Dose spectra based on the later data differed chiefly in the low energy region. The relative dose due to energy up to 100 kev averaged about 40 percent as compared to 12 percent in the above distribution. Three other dose distributions were calculated from Shot 4 and later Shot 1 data and are shown in Figures 4.1, 4.2, and 4.3. Figure 4.1, using the data of Table 4.2, is an extreme case with respect to the low energy component. All other samples for all the shots lie between this and Figure 4.2 of Reference 16. Figures 4.2 and 4.3 give the dose distributions for the H + 4.1 and H + 5.2 day times on the other Shot 1 sample. Figure 4.2 also indicates estimated error in portions below 0.3 Mev.

The dose spectra are all seen to group roughly into three regions with peaks at 100, 700, and 1500 kev. Since the spectra are those of 4 to 5 day old fission products, at which time the  $\text{Np}^{239}$  activity is at its greatest relative value, the low energy proportion due to this nuclide is higher than it was at H + 2 days when the  $\text{Np}^{239}$  component was still increasing (Figure 3.1). Based on this distribution, dosage and meter corrections for the low energy region during the exposure period are therefore generous. During the several days before and after this time the general spectrum shape apparently did not vary grossly in the higher energy regions. A total correction factor for the survey instruments was therefore calculated for each of these spectra and was assumed to hold for the period between fallout and surveys, as is described in Chapter 5.

TABLE 4.2 - Shot 4, H + 5.3 Days

Energy (Mev)	Percent of Flux	Cumulative Percent Dose
0 - 0.1	59.6	56
0.1 - 0.2	16.0	
0.2 - 0.3	8.1	70
0.4 - 0.5	4.6	76
0.6 - 0.7	4.3	
0.7 - 0.8	4.0	90
0.8 - 0.9	1.0	92
1.5 - 1.6	2.4	100

TABLE 4.3 - Shot 1, H + 4.1 Days

Energy (Mev)	Percent of Flux	Cumulative Percent Dose
0.100	0.548	31
0.200	0.136	
0.250	0.108	50
0.300	0.042	
0.486	0.037	65
0.659	0.055	
0.750	0.048	85
0.815	0.012	92
1.590	0.013	100

TABLE 4.4 - Shot 1, H + 5.2 Days

Energy (Mev)	Percent of Flux	Cumulative Percent Dose
0.035	5.97	10
0.65	11.53	
0.100	36.47	36
0.135	3.81	
0.210	10.49	
0.250	5.23	52
0.285	4.05	
0.320	2.21	
0.486	5.13	65
0.659	6.35	
0.750	5.06	83
0.815	1.82	89
1.590	1.88	100

#### 4.3 BETA ENERGY

The beta radiation energy was not measured directly in any of the fallout or soil samples. However, from available data on the radiochemical composition of the fallout (Reference 6), it has been estimated that from 30 to 65 percent of the beta radiation during the exposure period was due to  $\text{Np}^{239}$ , and had an average  $E_{\text{max}}$  of about 0.3 Mev. The balance of the radiation was of higher energy, with an average  $E_{\text{max}}$  of about 1.8 Mev. The half-value thickness in tissue for the low energy component is about 80 microns, with a range of about 800 microns total. For the high energy component, the half-value thickness is about 800 microns and the range about 8000 microns. Since no estimate could be made of the amount of material on the skin surface or length of time it remained there, only rough estimates based on clinical evidence could be made of the skin beta doses, (See Reference 16).

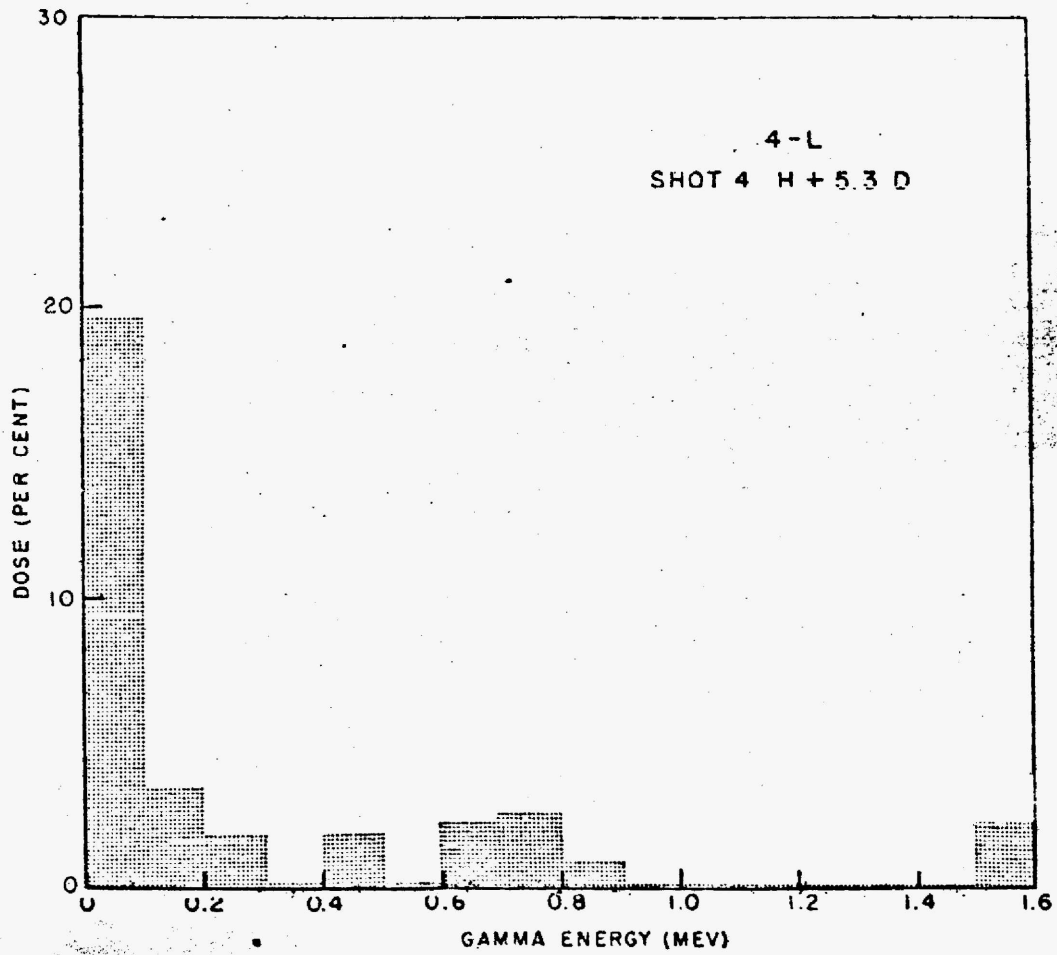


Fig. 4.1 Dose-Energy Distribution, Shot 4 H + 5.3 Day Sample

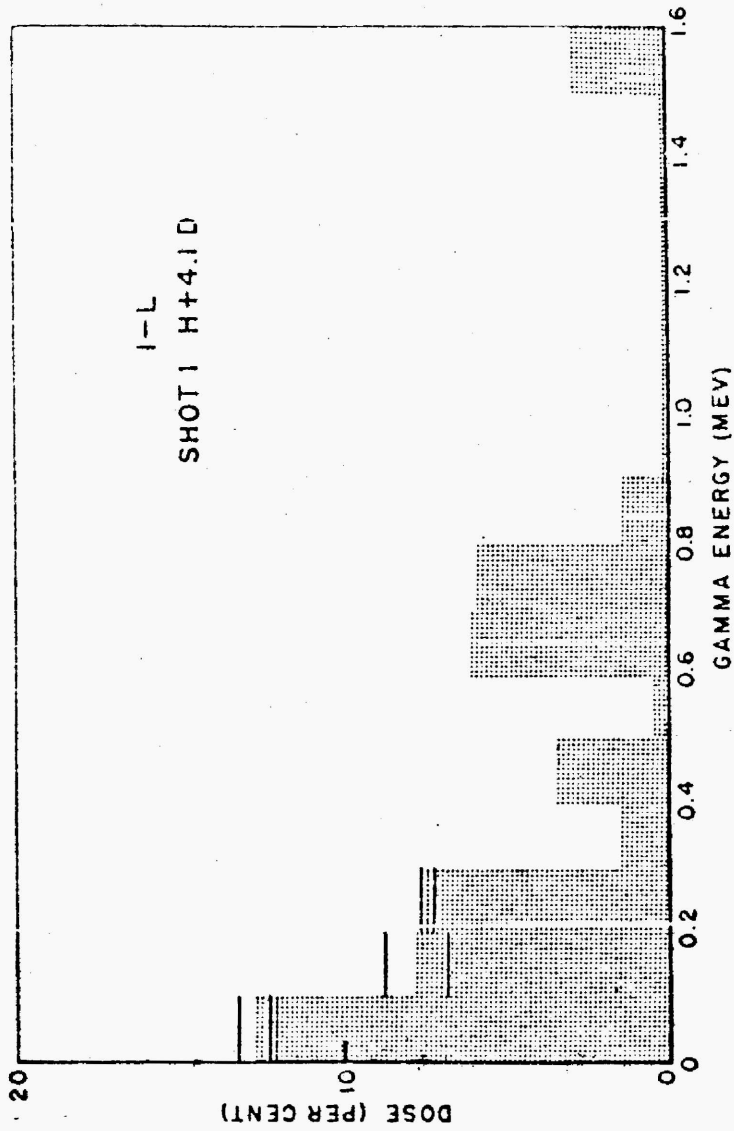


Fig. 4.2 Dose-Energy Distribution, Shot 1 H + 4.1 Day Sample

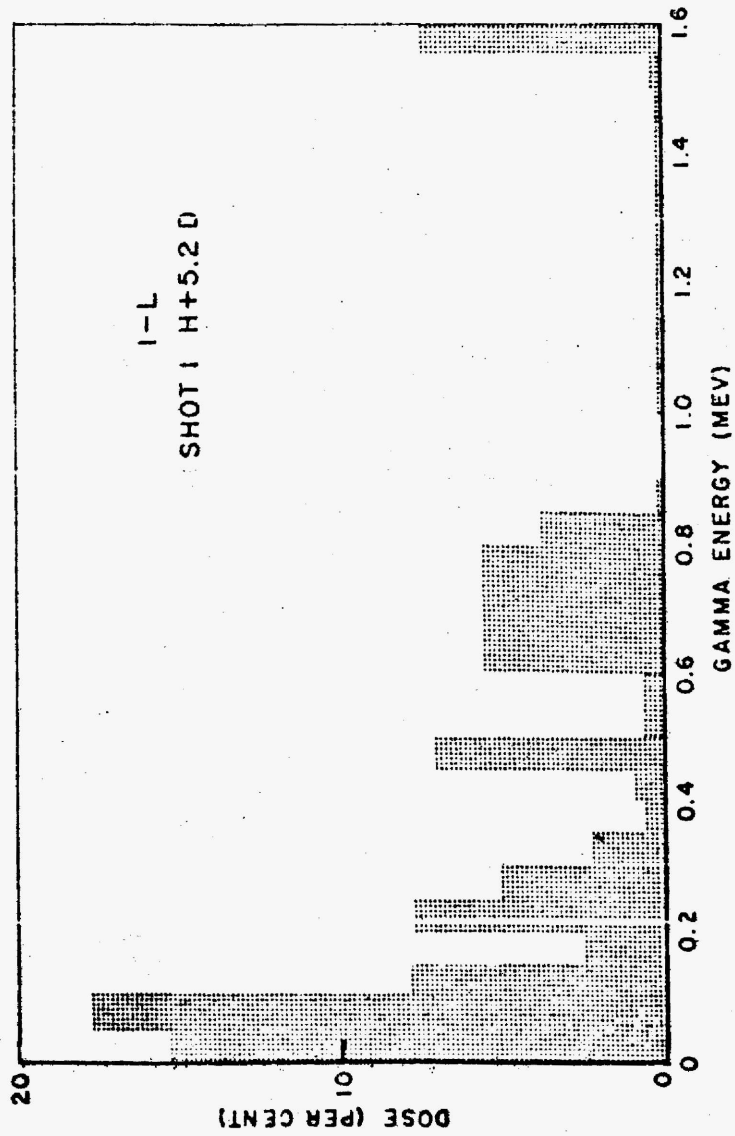


FIG. 4.3 Dose-Energy Distribution, Shot 1 H + 5.2 Day Sample

## CHAPTER 5

### METER RESPONSE FACTORS

#### 5.1 ENERGY RESPONSE

The response of the survey meter to the spectra calculated in Chapter 4 was evaluated in terms of a set of normalizing factors, one for each energy interval in the spectrum. By summing over the intervals and weighting each response factor by the fraction of total air-dose in that interval, a total response factor is obtained.

Thus, if  $D_i'$  is a dose reading for radiation of a given energy and  $k_i$  is the normalizing factor for that energy, then:

$$k_i D_i' = f_i D \quad (5.1)$$

Where:  $f_i$  = the fraction with the given energy of the total true dose  $D$ .

Hence:

$$D' = \sum D_i' = D \sum \frac{f_i}{k_i}$$

Solving for  $D$ :

$$D = \frac{D'}{\sum \frac{f_i}{k_i}} \quad (5.2)$$

The  $f_i$  may be taken from the dose-energy distributions in Chapter 4 and the  $k_i$  from Figure 5.1, which is a plot of the response factors found for the earlier model of the AN/PDR-39A, then called the AN/PMK-T1B (Reference 10). This is believed to be essentially identical in its response to the later models. For the spectrum used in the Reference 16 calculations, the total response factor was found to be 1.04. This value was used in the dose calculations of that report.

For the spectra shown in the Figures 4.1 to 4.3, the total energy response factors for all energies above 20 keV were found to be as given in Table 5.1. The value of 1.12 for the H + 5.2 day spectrum of Shot 1 (Figure 4.3) is used in the revised dose calculations of this report, since this spectrum represents the best data.

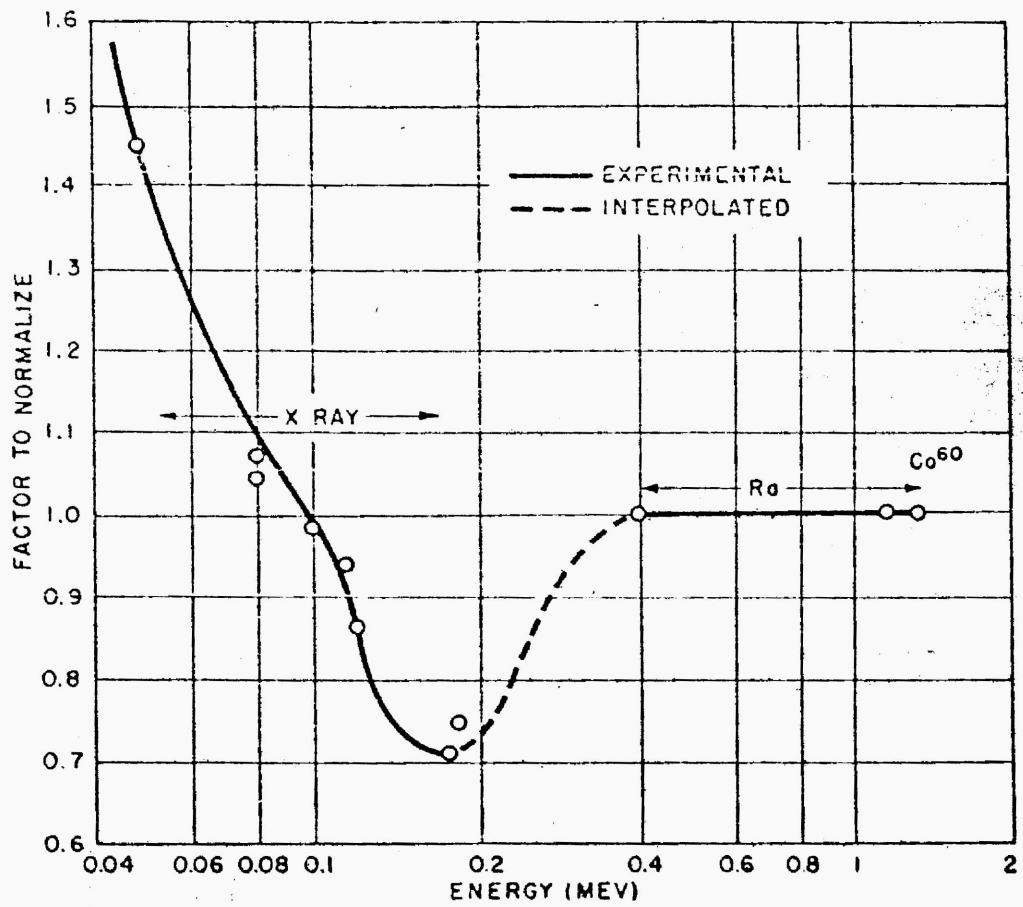


Fig. 5.1 Energy Response of Survey Meter AN/IDR-TLB

TABLE 5.1 - Total Energy Response Factors for AN/PDR-37A

Spectrum Shape	Total response Factor
Shot 4 (4-L) H + 5.3 Days (Figure 4.1)	1.17
Shot 1 (1-L) H + 4.1 Days (Figure 4.2)	1.06
Shot 1 (1-L) H + 5.2 Days (Figure 4.3)	1.12
Shot 1 (1-L) H : 94 Hours (Figure 4.2 of Reference 16)	1.04

## 5.2 GEOMETRY RESPONSE

The response of the instrument is known to vary also with the direction of incidence of the flux, but no allowance was made for this factor in Reference 16. An attempt has been made to correct for this effect by using the plots shown in Figure 5.2. This figure, taken from Reference 10, is a graphical representation of the directional response to a 10-mg Radium source of a 11B instrument in the horizontal and in two vertical planes. It was felt to be sufficiently accurate to make the approximation shown in the graph by setting a straight line limit to the response vector in one region and, further, to assume that the response is cylindrically symmetric about the XX' axis. Maximum sensitivity, indicated by a vector length of unity, is then in the OX direction on the XX' axis. If a flux (F) per unit solid angle impinges on the instrument at an angle  $\theta$  with respect to OX', the reading on the meter will be (assuming that the response is linearly proportional to flux intensity):

$$D' = rD = rkF \quad (5.3)$$

where:  $k$  = proportionality constant  
 $D$  = "true" air-dose  
 $r$  = vector response factor

By the above approximation, the vector response factor ( $r$ ) is given by:

$$\begin{aligned} 0 \leq \theta \leq \cos^{-1} \frac{1}{2} = \pi/3 & : r = 0.6 \sec \theta \\ \pi/3 \leq \theta \leq \pi & : r = 1 \end{aligned} \quad (5.4)$$

The average value of  $r$  is given by:

$$\bar{r} = \frac{\int_0^\pi r d\theta}{\int_0^\pi d\theta} \quad (5.5)$$

Using the above values of  $r$ ,  $\bar{r} = 0.92$ ; i.e., the instrument is about 92 percent efficient. Thus the average directional response correction factor is 1.09, implying that the reading inside a homogeneous cloud or over a homogeneous plane source is about 9-percent low for this average energy, which is roughly in the 1-Mev region.

For the very low energy component below 100 kev, it is not known whether the relative directional response varies grossly from the above. It is assumed here that it does not. The doses calculated in this report are therefore based on this directional correction. Combining this geometry factor with the energy correction of Table 5.1 for the H + 5.2 day spectrum and Shot 1, a total correction factor of 1.22 results which was used in the air-dose calculations in Section 6.1 of this report.

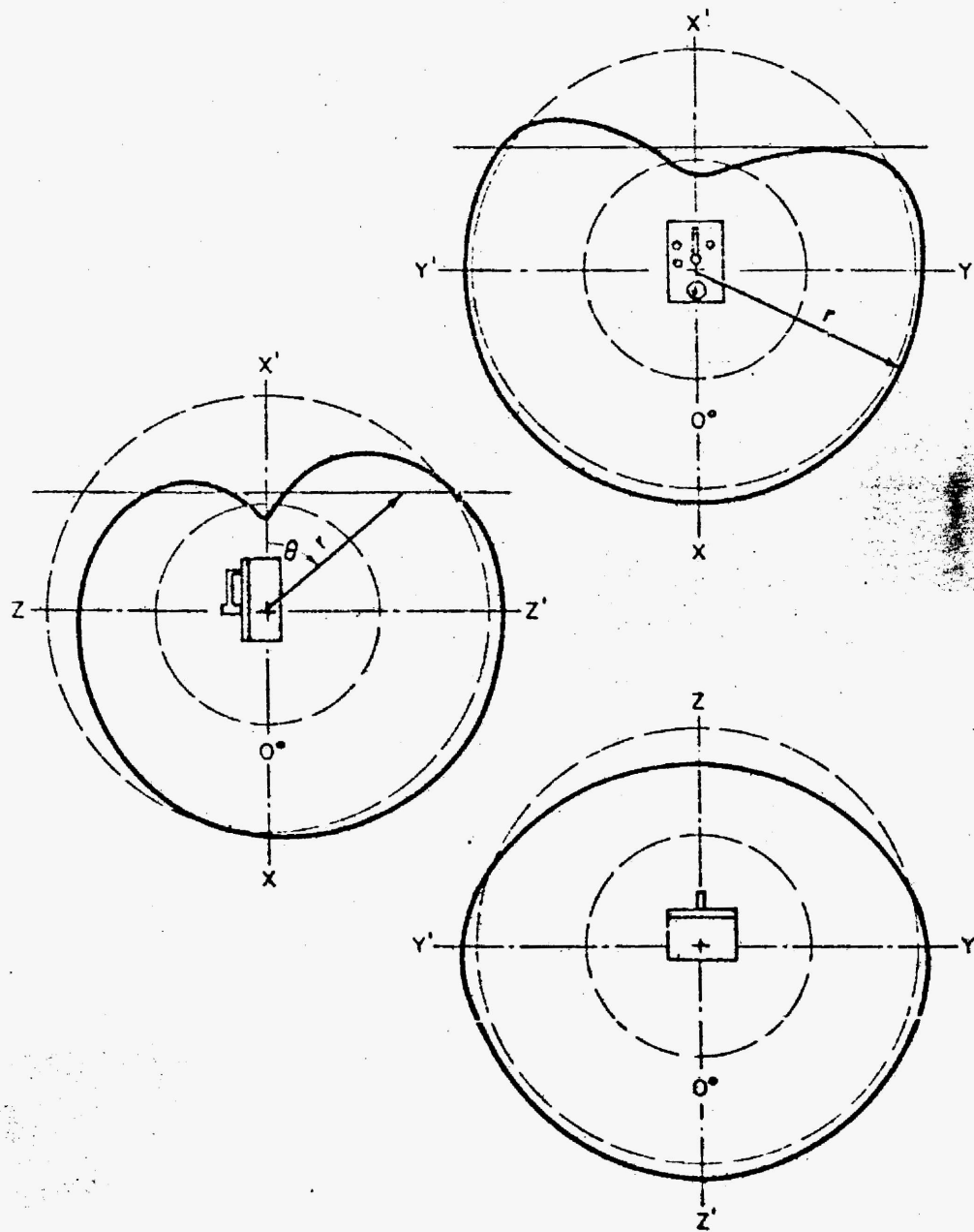
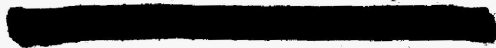


Fig. 5.2 Directional Response of Survey Meter M/PDR-11B



## CHAPTER 6

### DURATION AND TIME DISTRIBUTION OF DOSES

#### 6.1 AVAILABLE DATA

In Chapter 2, the only existing field data on dose rates and total dose are summarized. The information does not provide answers to two important questions: (1) what was the time for each island at which the fallout cloud arrived; i.e., when did the radiation level on each of the islands rise above the normal background and (2) how steeply and for how long did the radiation-level rise before it reached its maximum value and decayed away at the rate determined by its own composition (discussed in Chapter 3); i.e., how heavy was the fallout at any time it was occurring and how long did it last? Since only the times of evacuation were directly known, assumptions on both these questions were basic to an estimate of total dose.

It would have been desirable to have had an instrument on at least one of the islands capable of recording enough data to answer these questions. As it is, it was fortunate that there was even a low-level monitoring instrument in operation on Rongerik (Table 2.1), although its full scale capacity was soon exceeded by the rapidly increasing dose rate of the fallout. The time at which the fallout began was at least quite definitely established on Rongerik and it coincided with the time at which the snow-like material was first seen.

For the other islands, therefore, the times at which similar material had been seen to commence falling could be taken as the beginning of the radiation exposure times. It only remained to determine what these times had been.

Questioning the inhabitants of the other islands resulted in a group of estimates of arrival time which were in fairly good agreement, though the manner of questioning sometimes appeared to influence the answers. However the times estimated in this fashion were quite close to those resulting from other information; i.e., the wind velocities at the time, the time of beginning fallout on Rongerik, and the relative distances of the other islands from Bikini. Only on Utirik was no actual observation of the fallout made; the estimate of arrival time there was made using only the time of arrival on Rongerik and the wind-and-distance-factors. The values of fallout and evacuation times used are summarized in Table 6.1.

TABLE 6.1 - Fallout and Evacuation Times

Island	Estimated Initial Fallout Times (hours)	Evacuation Time (hours)
Rongerik	H + 6.8	H + 23.5 (6 men) H + 34 (20 men)
Rongelap	H + 4	H + 50 (16 people) H + 51 (48 people)
Allinginae	H + 4	H + 58
Utirik	H + 22	H + 55 to H + 78

## 6.2 ESTIMATES OF FALLOUT DURATION

The rate of increase of radiation intensity, the time at which it reached its maximum level due to decrease of fallout, and the total duration of the fallout can only be estimated on circumstantial grounds. The data of Table 2.1 for Rongerik are not sufficient to warrant an extrapolation over two orders of magnitude. It is unlikely that the increase of intensity was simply linear either on Rongerik or any of the other islands. But, if the rate of increase is assumed constant and extrapolated to a point for which subsequent decay alone would reduce the dose rate to the values found at later times, a fallout time of 16 hours on Rongerik, for example, is found to be a necessary consequence (Curve a, Figure 6.1). That is to say, 16 hours would have elapsed at such a constant fallout dose rate increase before the time of maximum dose rate on the island would have occurred - the time at which the fallout was increasing the radioactivity level at the same rate that radioactive decay was reducing it. For such a constant build up, this equality would have occurred only for an instant, (Point A<sub>1</sub>), after which the fallout would have suddenly ceased.

The actual fallout must, of course, have had a variable rate of increase and decrease, reaching a maximum and gradually decreasing to the rate governed by decay alone. However, using the initial rate of increase and drawing a more gradual maximum would place the cessation of the fallout at an even later time (Curve b, Point A<sub>2</sub>). Since the visible fallout is believed to have ceased sometime after midnight on 1 March or at about H + 18 hours (Point A<sub>3</sub>), an increase in the rate of increase after a short time was almost certainly the case (Curves c, d, and e). But the steepness of this rate of increase, the sharpness of the maximum point and the gradualness of the fallout diminution are unknown, so that there is no direct evidence to show whether Curve c or Curve e, for instance, is closer to representing the event.

There are, however, indirect indications. Monitor data from previous nuclear events have indicated that a radioactive cloud is not

uniformly high in activity throughout, the first portion being the most intense and the balance tailing off. Initially heavy fallout has been reported to produce a peak of airborne radioactivity soon after its arrival, with the airborne activity level then decreasing. The latter part of a fallout, though still observable as dust, may then add only a small fraction to the total dose due both to aerosol and material already on the ground, especially if radioactivity was mainly confined to the larger particles which fell out most quickly. If this is the case, the total phenomenon would tend toward the effect of a shorter fallout, and the total dose would then be best estimated by assuming the fallout to have been complete in some shorter "effective" time, such as Curve f.

The Kangerik film badge data in Table 2.3 may be used to derive such an effective fallout time estimate. This procedure was followed. The decay rate, energy spectrum, and meter response discussed in Chapters 3 and 5 were used and the later dose rate measurement on Kangerik (Table 2.4) was taken as a starting point. The upper limit of dose found with the outdoor badge readings (approximately 100 r Table 6.1) then resulted from assuming a 12-hour "effective constant fallout" time. This was, therefore, taken as a most probable time and the resulting straight line midway between Curves a and f in Figure 6.1 was used in calculating the probable 12-hour dose for each island (Curve g). Though this estimate differs appreciably from that of 1 hour which was originally used as an effective time in Reference 16, the later spectrum, decay rate, and meter response estimates made a 12-hour value more plausible if the film badge readings were accepted.

Keeping a 1-hour assumption would have resulted in a dose some 50 percent higher than the outdoor badge readings showed. Since the accuracy of the film badge readings was believed to be better than 50 percent, the 12-hour value was therefore used, as it is more consistent with all the other available information. Nevertheless, the duration of fallout still remains the least known parameter of the exposures.

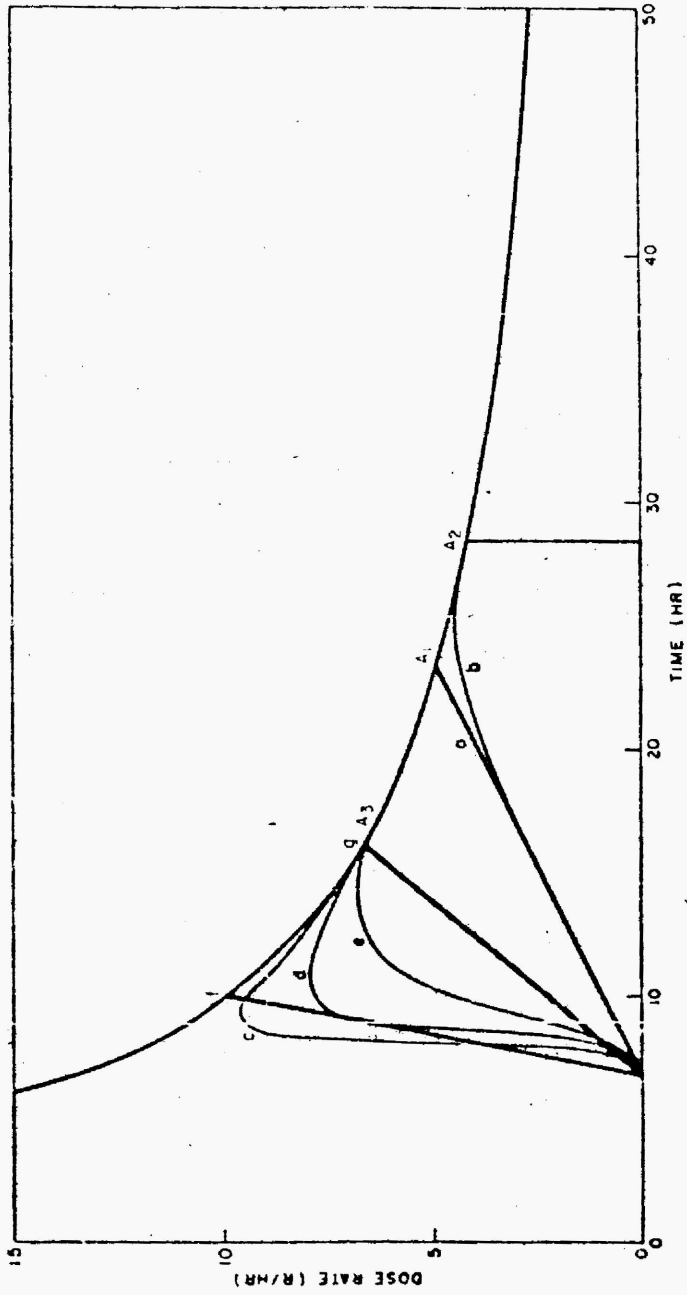


Fig. 6.1 Fallout Dose Rate Versus Time Estimates, Pasco, Idaho

## CHAPTER 7

### EXPOSURE GEOMETRY EFFECTS

#### 7.1 DISCUSSION

In clinical and laboratory exposures, the radiation flux usually follows a narrow beam or at least a point-source "divergent" geometry. When an air-dose is used to specify the exposure conditions for a thick target, it is generally measured at the point subsequently occupied by the center of the proximal surface of the patient or experimental animal with respect to the source. For field exposures such as occurred on the islands, the radiation source is not a point and the exposure geometry is "diffuse" rather than "divergent."

When a cloud or a large planar area is the source, all surfaces of the irradiated individual are "proximal," in the sense that the air-dose measured anywhere in the space subsequently occupied by the individual is the same. It is this air-dose which is measured by a field instrument; it does not bear the same relationship to the skin dose and depth dose as does the air-dose measured in a point source geometry. If a bilateral exposure is made in the laboratory, one-half the dose is usually given with one side of the individual facing the source and one-half with the other. This is a closer approach to the field geometry. But, if the air-dose has been measured at the center of the proximal surface as above, it is still not related to the depth dose in the same way as is the field air-dose.

The doses received by the individuals on the islands were from both the cloud itself and the fallout deposited on the ground. It is believed likely, as discussed in Chapter 6, that the cloud dose was only a small part of the total dose and that the dose from the plane ground source contributed the major portion. This corresponds to the assumption of early maximum activity and short effective fallout time which was made in Chapter 6 for the maximum dose case. Alternatively, if a long fallout actually occurred, the source would have remained a cloud longer and the cloud volume, rather than the surface distribution, would have accounted for more of the total dose. In either case, it would appear that the midline dose, rather than the dose measured in air, would be the better common parameter in terms of which to predict biological effect. Since most existing data tacitly assumes narrow beam geometry, this distinction becomes important in relating field air-doses and their consequences to known clinical or experimental results (References 11, 12).

## 7.2 EXPERIMENTAL SIMULATION AND GEOMETRY FACTOR

In such a diffuse field, the decrease of dose with depth in tissue is less pronounced than that resulting from a bilateral exposure to an X-ray beam and the relationship to air-dose differs as noted in the two cases. The result is that, for a given energy, the dose at the center of the abdomen is considerably higher than a given proximal air-dose would imply for the narrow-beam or point-source case.

Figure 7.1 illustrates the depth dose curve in a 36-cm diameter cylindrical masonite phantom from an experimental simulation of the field geometry (Reference 13) using a spherically oriented group of 36  $\text{Co}^{60}$  sources. The phantom was placed at the center of the assembly. This is compared to a conventional bilateral depth-dose curve measured in the same phantom and obtained with a single  $\text{Co}^{60}$  source. Both are normalized to air-dose, but the average air-dose at all points later occupied by the phantom surface is implicit for the diffuse case, while the proximal air-dose is used in the bilateral case.

Figure 7.2 is a similar comparison for 200-KVP, 0.5-mm, copper-filtered X-rays, with the diffuse geometry that of a plane rather than spherical source assembly. This was produced in this case by rotation of the phantom and ion chamber in the beam of a stationary X-ray unit. The useful beam angle of the unit was wide enough to include the whole phantom. The average air-dose around the circumference was here used for the diffuse geometry and the proximal air-dose again in the bilateral exposure. It is evident that for both these energies (the effective energy of the X-ray beam being about 90 KV), the diffuse-narrow beam depth dose ratio for either  $2\pi$  radians (plane) or  $4\pi$  steradians (volume) diffuse geometry is almost the same. That is, the midline dose is about 50 percent higher and the 5-cm dose is 35 percent higher than the same air-dose (measured proximally) would imply in the narrow beam bilateral exposure. It is therefore assumed that this approximate factor will apply throughout the field exposures.

On this basis the air-dose values calculated from the survey meter readings (Table 8.1) should be multiplied by 1.5 in order to compare the situation to that of a bilateral exposure to a source with the same energy distribution but using a point source geometry and a proximally measured air-dose. Alternatively, if a point source of higher energy, say  $\text{Co}^{60}$ , were used bilaterally in the same way to simulate a field exposure to only the higher gamma components, then the meter energy correction factor would be unity. In this case, to specify a bilateral exposure yielding a midline dose equal to that with diffuse geometry, the point source air-dose should be the diffuse field air-dose measured with the meter and multiplied by  $(1.09 \times 1.5)$  only.

The doses are discussed further in Chapter 8.

882 019

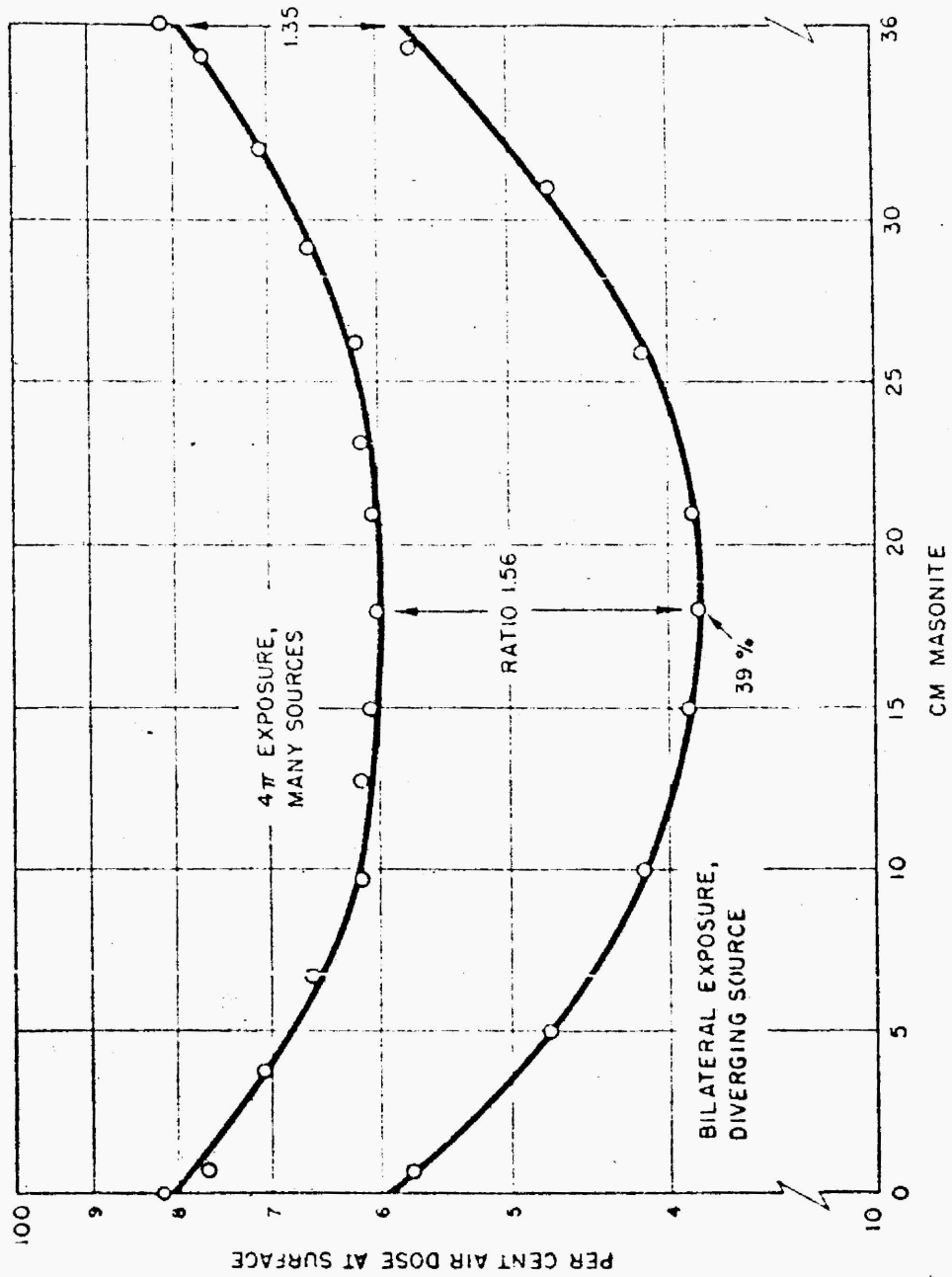


Fig. 7.1 Depth-Dose Curves, 36-cm Flinton, 1.2 MeV

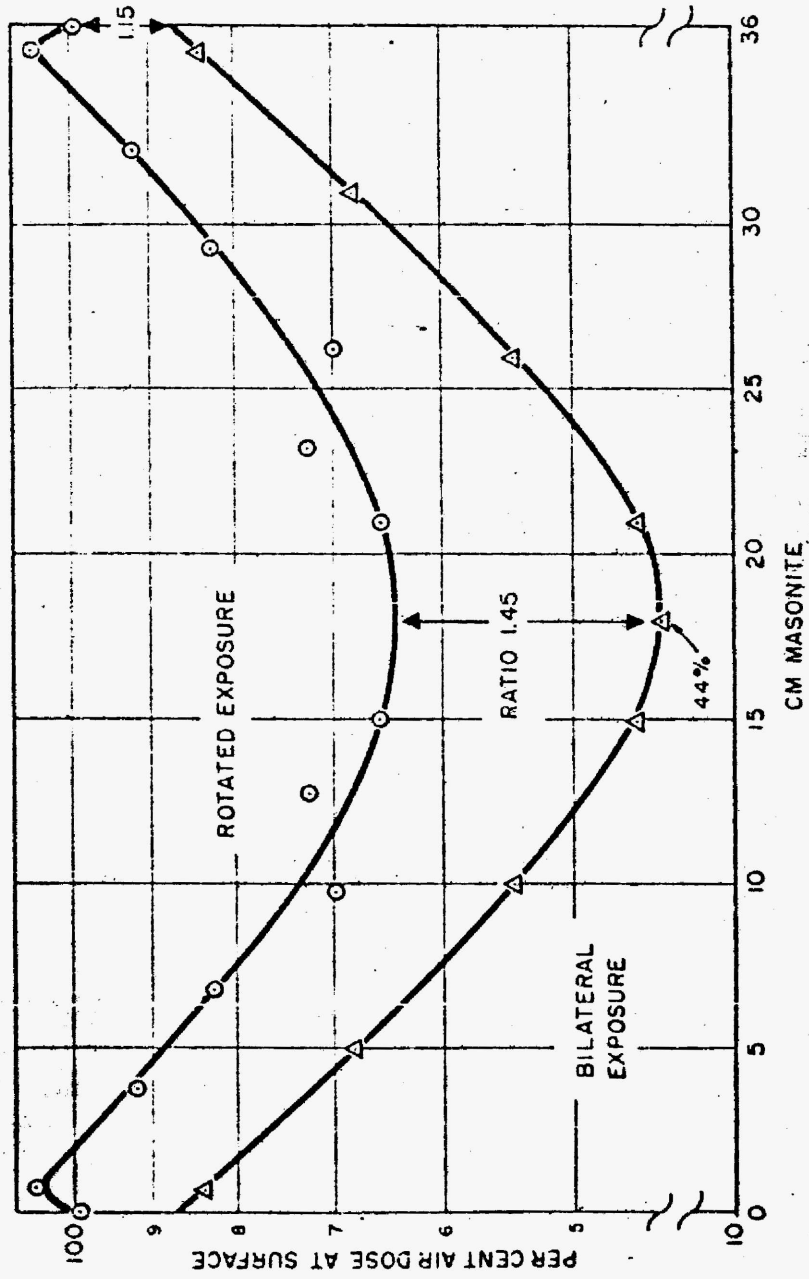


Fig. 7.2 Depth-Dose Curves, 36-cm Phantoms, 200 kVp

## CHAPTER 8

### TOTAL DOSE ESTIMATES

#### 8.1 CALCULATED VALUES

The total doses calculated for each of the islands for hypothetical fallout times of 8, 12, and 16 hours are given in Table 8.1, together with the doses calculated in Reference 16, in order to illustrate the difference in the estimates due to the later information on gamma spectra, meter response, and decay rates.

The 12-hour fallout value is considered most probable, being most consistent with the Rongerik film badge data (see Section 6.2). Doses based on this value are multiplied by the geometry factor discussed in Chapter 7, in order to express them in terms of the air-dose from a source of similar energy under bilateral exposure laboratory conditions which would have produced the same midline dose. A plot of dose rate versus time based on Figure 3.3 was used and the total dose was graphically determined by normalizing ordinates and dose rates for a given time and measuring the area under curves similar to Figure 6.1. This was done assuming all three fallout times for each island.

The air-dose rates measured at later times (Table 2.4) were multiplied by the total correction factor for geometry and energy dependence of the survey meter (see Section 5.2). Fallout beginning times and evacuation times used were those of Table 6.1. It was found that doses calculated using the decay exponents of Section 3.2 were in good agreement with those determined graphically.

#### 8.2 DISCUSSION

Figure 8.1 illustrates the cumulative air-dose as a function of time on Rongelap atoll, based on the 12 hour fallout assumption. It can be seen that the rate of delivery of the dose varied continuously, the major portion being received at the higher dose rate prevailing in the mid-portion of the exposure period. By the time that 90 percent of the dose had been received at  $H + 43$  hours, for example, the dose rate had fallen to 2.7 r/hr, less than 40 percent of its maximum value of 7.4 r/hr at  $H + 16$  hours. At  $H + 16$  hours, 25 percent of the dose had been received. Thus the dose rate during exposure differed markedly from that usually encountered using X-ray units.

The dose values for Rongerik given in Table 8.1 are 75 percent of the computed values, averaged for the 20.5- and 34-hour exposures. This

was felt to best express the average air-dose received by personnel who spent roughly half their time inside structures where the dose rate was later found to be roughly half that outdoors. On the other islands no such shielding was present, and no reduction factor was applied. The same procedure was followed for all the calculations.

TABLE 8.1 - Total Gamma Doses

Island	Dose 3-Hour Fallout (r)	12-Hour Fallout (r)	16-Hour Fallout (r)	Ref. 16 (r)	12-Hour Bilateral Air-dose (Point Source of Same Energy) for Equal Midline Dose (r)
Rongerik*	106	86	70	78	130
Rongelap	209	182	159	175	270
Ailinginae	92	81	72	69	120
Utirik	15	13	12	14	20

\*See Section 8.2

### 8.3 SOFT GAMMA AND BETA COMPONENTS

In addition to the total body gamma dose, the very soft gamma and higher energy beta radiation from the plane source contributed to the skin dose. Further skin irradiation resulted from local deposits of fallout material on the body surface itself. The latter is impossible to estimate, but the former may be roughly attempted as follows.

The beta dose rate in air at a height of 3 feet above the surface of an infinite plane contaminated with mixed 24-hour-old fission products is estimated to be about three times the air gamma dose (Reference 14). The midline gamma dose is approximately 60 percent of the portion of the air gamma dose due to 100-KV radiation or above (Reference 13). This portion, in turn, is estimated to be 60 percent of the corrected gamma dose measured in air by a calibrated instrument. Thus, the dose at the surface of a phantom exposed to mixed fission product radiation from an external plane source might be expected to be about eight times  $(3/(0.6)^2)$  the midline dose, if both occur at 3 feet off the ground.

Such a depth-dose measurement has in fact been made experimentally at a previous field test (Reference 15), using a phantom man exposed to both the initial and residual radiation. The depth-doses for each situation are shown in Figure 8.2 with all data as percent of the 3-cm dose. With the diverging initial radiation from the point of explosion, the exit dose was seen to be 63 percent of the 3-cm dose. But, with the diffuse residual field of fission product radiation, a surface dose

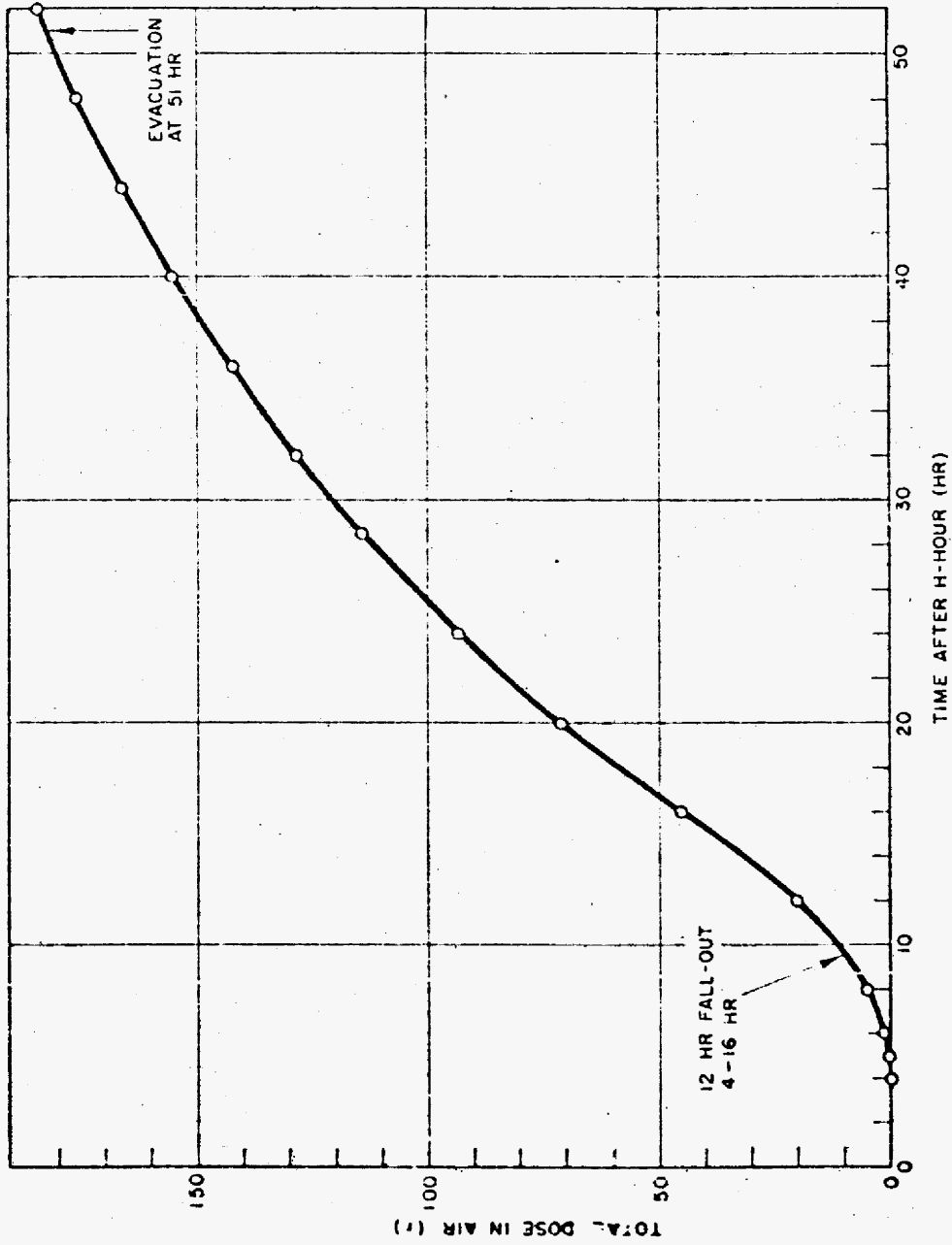


Fig. 8.1 Cumulative Air-Dose with Time, Rongelap Atoll.

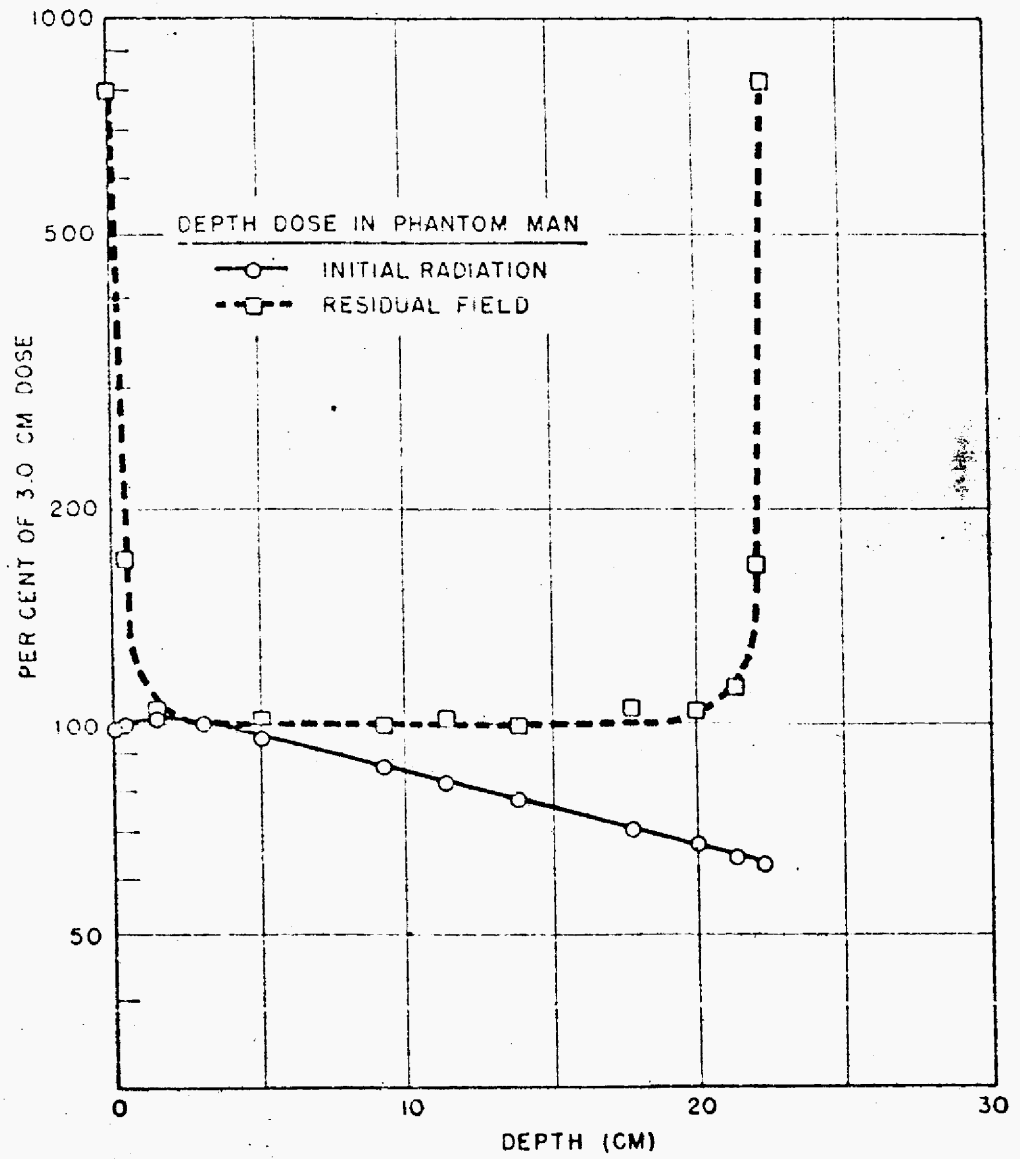


Fig. C.2 Field Depth-dose Measurement, Operation UFGICT-1101HOLE

some eight times greater than the 3-foot-and-deeper dose from the harder gamma components was observed. This is seen to be of the same order of magnitude as that estimated above.

At heights above and below the 3-foot level, this surface dose would become lower and higher, respectively. But, since it is due to soft radiation of short range, it probably would not exceed 50 times the 3-foot air gamma dose or 80 times the midline dose, even in contact with the ground.

An estimate of skin dose due to ground contamination for the Rongelap case would result, for example, in a figure of about 2000 rep to the dorsum of the foot, 600 rep at the hip level, and 300 rep at the head if continuous exposure with no shielding occurred. Some reduction in dose undoubtedly resulted from shielding and movement and it seems probable that the external beta dose from local skin contamination far outweighed in importance that from the ground. This is emphasized by the probability that clothing reduced the beta dose from the ground by 10 to 20 percent.

## CHAPTER 9

### CONCLUSIONS

The AN/PLR-39A is estimated to require a correction factor of about plus 20 percent in dose-rate readings made under the conditions discussed.

The decay of the radioactivity of the fallout during the exposure period is believed to be expressible by the factor  $T^{-0.83}$ .

The external gamma dose was delivered primarily by radiation energies of 100, 700, and 1500 kev. The beta dose was believed to be delivered by beta radiation of maximum energies of 0.3 and 1.8 Mev, mostly from fallout deposited on the skin itself.

The exposures occurred between 4 and 78 hours after the detonation. The fallouts were probably of about 12-hours duration.

Diffuse source geometry increased the midline dose by about 50 percent compared to the midline dose which would have resulted from a bilateral narrow beam exposure of the same air-dose.

Error in the estimates is believed to be less than 50 percent.

Total air gamma doses are estimated as follows: Rongerik, 86 r; Rongelap, 182 r; Ailinginae, 81 r; and Utirik, 13 r.

## REFERENCES

1. Cohn, S. H. et al; Addendum Report, Project 4.1, WT-936, Operation CASTLE; OFFICIAL USE ONLY.
2. Maupin, C. E.; Private Communication; AMSRGS, Walter Reed Army Medical Center, Washington, D. C.
3. Rad Safe Narrative Sequence of Events; Memo for Record, BRAVO Shot, Operation CASTLE; Hqs JTF-7, Washington, D. C.
4. Scoville, H. et al; Report of the Radiological Safety Group; USNRDL ltr 0010755, 12 March 1954; Hdqtrs JTF-7 Rpt No. TU-13-54-375; SECRET-RD.
5. Tompkins, E. R. et al; Chemical, Physical, and Radiochemical Characteristics of the Contaminant; Project 2.6a, WT-917, Operation CASTLE; SECRET-RD.
6. Ballou, N. E.; Private Communication. Also: Hunter, H. F. and Ballou, N. E.; Fission Product Decay Rates; Nucleonics, 9:5, 1951.
7. Gates, L. G. and Eisenhauer, C.; Spectral Distribution of Gamma Rays Propagated in Air; Tech Analysis Report 502A, January, 1954.
8. Cook, C. S. et al; Gamma Ray Spectral Measurements of Fallout Samples from Operation CASTLE; USNRDL-TR-32, 1955.
9. Mather, R. L.; USNRDL ltr 0010709, 17 June 1954; SECRET-RD.
10. Turke, J. K. and Reardon, D. A.; Evaluation of the AN/PDR-TLB Gamma Survey Meter; USNRDL Instrument Evaluation Report NE 051555, October 1951.
11. Tullis, J. L. et al; Mortality in Swine and Dose Distribution Studies in Phantoms Exposed to Supervoltage Roentgen Radiation; Amer. J. Roent. Rad. Ther. Nucl. Med., 47, 620-627, 1952.
12. Tullis, J. L. et al; Mortality in Swine Exposed to Gamma Radiation from an Atomic Bomb Source; Radiol., 62, 409-15, 1954.
13. Sondhaus, C. A.; Unpublished Data.
14. Teresi, J. D. and Brodlo, A.; Discussion of the Ratio of Beta Surface rep Dose to Gamma Dose Associated with Fission Product Contamination; USNRDL-TM-2, 1954; CONFIDENTIAL-RD.
15. Chambers, F. W. et al; Unpublished Data; AMRI, Operation UPSHOT-KNOTHOLE.
16. Cronkite, E. P. et al; Study of Response of Human beings Accidentally Exposed to Significant Fallout Radiation; Project 4.1, WT-923, Operation CASTLE, October 1954; CONFIDENTIAL.

# UNCLASSIFIED

## DISTRIBUTION

Military Distribution Category 5-70

### ARMY ACTIVITIES

- 1 Asst. Dep. Chief of Staff for Military Operations, D/A, Washington 25, D.C. ATTN: Asst. Executive (H&M)
- 2 Chief of Research and Development, D/A, Washington 25, D.C. ATTN: Special Weapons and Air Defense Division
- 3 Chief of Ordnance, D/A, Washington 25, D.C. ATTN: ORDT&AP
- 4-6 Chief Signal Officer, D/A, I&O Division, Washington 25, D.C. ATTN: DS&AF
- 7 The Surgeon General, D/A, Washington 25, D.C. ATTN: Chief, I&O Division
- 8-9 Chief Technical Officer, D/A, Washington 25, D.C.
- 10 The Quartermaster General, D/A, Washington 25, D.C. ATTN: Research and Development Div.
- 11-14 Chief of Engineers, D/A, Washington 25, D.C. ATTN: CE&NS
- 15 Chief of Transportation, Military Planning and Intelligence Div., Washington 25, D.C.
- 16-18 Commanding General, Continental Army Command, Ft. Monmouth, Va.
- 19 President, Board #1, Headquarters, Continental Army Command, Ft. Hill, Calif.
- 20 President, Board #2, Headquarters, Continental Army Command, Ft. Knox, Ky.
- 21 President, Board #3, Headquarters, Continental Army Command, Ft. Benning, Ga.
- 22 President, Board #4, Headquarters, Continental Army Command, Ft. Bliss, Tex.
- 23 Commanding General, First Army, Governor's Island, New York 4, N.Y.
- 24 Commanding General, Second Army, Ft. George G. Meade, Md.
- 25 Commanding General, Third Army, Ft. McPherson, Ga. ATTN: ACOFS, G-3
- 26 Commanding General, Fourth Army, Ft. Sam Houston, Tex. ATTN: G-3 Section
- 27 Commanding General, Fifth Army, 1660 N. Hyde Park Blvd., Chicago 15, Ill.
- 28 Commanding General, Sixth Army, Presidio of San Francisco, Calif. ATTN: ANACT-4
- 29 Commanding General, U.S. Army Caribbean, Ft. Anador, C.R. ATTN: Cal. Off.
- 30 Commanding General, USARFANT & MORN, Ft. Brooke, Puerto Rico
- 31 Commanding General, Southern European Task Force, APO SF, New York, N.Y. ATTN: ACOFS, G-3
- 32-33 Commander-in-Chief, Far East Command, APO 500, San Francisco, Calif. ATTN: ACOFS, G-3
- 34 Commanding General, U.S. Army Forces Far East (Main), APO 343, San Francisco, Calif. ATTN: ACOFS, G-3
- 35 Commanding General, U.S. Army Alaska, APO 942, Seattle, Wash.
- 36-37 Commanding General, U.S. Army Europe, APO 903, New York, N.Y. ATTN: COMT Div., Casual Dev. Br.
- 38-39 Commanding General, U.S. Army Pacific, APO 954, San Francisco, Calif. ATTN: Cal. Off.
- 40 Commandant, Command and General Staff College, Ft. Leavenworth, Kans. ATTN: ALM, A-7
- 41 Commandant, Army War College, Carlisle Barracks, Pa. ATTN: Library
- 42 Commandant, The Artillery and Guided Missile School, Ft. Gill, Okla.
- 43 Secretary, The Antiaircraft Artillery and Guided Missile School, Ft. Bliss, Texas. ATTN: Maj. George L. Alexander, Dept. of Defense and Command Arms
- 44 Commanding General, Army Medical Service School, Brooks Army Medical Center, Ft. Sam Houston, Texas
- 45 Director, Special Weapons Development Office, Headquarters, CONARC, Ft. Bliss, Tex. ATTN: Capt. T. E. Skinner

- 46 Chief, Joint Chief of Staff for Research, Center Head Army Medical Center, and Institute, D.C. Department of the Army, William H. Rorer, West Point, N.Y. ATTN: Chief of Staff
- 47 Commanding General, 1st Cavalry Division, 1st Cavalry Division, Ft. Benning, Ga.
- 48-50 Commanding General, 1st Infantry Division, 1st Infantry Division, Ft. Benning, Ga.
- 51-53 Commanding General, 2nd Infantry Division, 2nd Infantry Division, Ft. Benning, Ga.
- 54 Commanding General, 3rd Infantry Division, 3rd Infantry Division, Ft. Benning, Ga.
- 55 Commanding General, 4th Infantry Division, 4th Infantry Division, Ft. Benning, Ga.
- 56 Commanding General, 5th Infantry Division, 5th Infantry Division, Ft. Benning, Ga.
- 57 Commanding General, 6th Infantry Division, 6th Infantry Division, Ft. Benning, Ga.
- 58 Commanding General, 7th Infantry Division, 7th Infantry Division, Ft. Benning, Ga.
- 59 Commanding General, 8th Infantry Division, 8th Infantry Division, Ft. Benning, Ga.
- 60 Commanding General, 9th Infantry Division, 9th Infantry Division, Ft. Benning, Ga.
- 61 Commanding General, 10th Infantry Division, 10th Infantry Division, Ft. Benning, Ga.
- 62 Commanding General, 11th Infantry Division, 11th Infantry Division, Ft. Benning, Ga.
- 63 Commanding General, 12th Infantry Division, 12th Infantry Division, Ft. Benning, Ga.
- 64 Commanding General, 13th Infantry Division, 13th Infantry Division, Ft. Benning, Ga.
- 65 Commanding General, 14th Infantry Division, 14th Infantry Division, Ft. Benning, Ga.
- 66 Commanding General, 15th Infantry Division, 15th Infantry Division, Ft. Benning, Ga.
- 67 Commanding General, 16th Infantry Division, 16th Infantry Division, Ft. Benning, Ga.
- 68 Commanding General, 17th Infantry Division, 17th Infantry Division, Ft. Benning, Ga.
- 69 Commanding General, 18th Infantry Division, 18th Infantry Division, Ft. Benning, Ga.
- 70 Commanding General, 19th Infantry Division, 19th Infantry Division, Ft. Benning, Ga.
- 71 Commanding General, 20th Infantry Division, 20th Infantry Division, Ft. Benning, Ga.
- 72 Commanding General, 21st Infantry Division, 21st Infantry Division, Ft. Benning, Ga.
- 73 Commanding General, 22nd Infantry Division, 22nd Infantry Division, Ft. Benning, Ga.
- 74 Commanding General, 23rd Infantry Division, 23rd Infantry Division, Ft. Benning, Ga.
- 75-76 Commanding General, 24th Infantry Division, 24th Infantry Division, Ft. Benning, Ga.
- 77 Commanding General, 25th Infantry Division, 25th Infantry Division, Ft. Benning, Ga.
- 78 Commanding General, 26th Infantry Division, 26th Infantry Division, Ft. Benning, Ga.
- 79-80 Commanding General, 27th Infantry Division, 27th Infantry Division, Ft. Benning, Ga.
- 81 Commanding General, 28th Infantry Division, 28th Infantry Division, Ft. Benning, Ga.
- 82 Commanding General, 29th Infantry Division, 29th Infantry Division, Ft. Benning, Ga.
- 83 Commanding General, 30th Infantry Division, 30th Infantry Division, Ft. Benning, Ga.
- 84 Commanding General, 31st Infantry Division, 31st Infantry Division, Ft. Benning, Ga.
- 85 Commanding General, 32nd Infantry Division, 32nd Infantry Division, Ft. Benning, Ga.
- 86 Commanding General, 33rd Infantry Division, 33rd Infantry Division, Ft. Benning, Ga.
- 87 Commanding General, 34th Infantry Division, 34th Infantry Division, Ft. Benning, Ga.
- 88 Commanding General, 35th Infantry Division, 35th Infantry Division, Ft. Benning, Ga.
- 89 Commanding General, 36th Infantry Division, 36th Infantry Division, Ft. Benning, Ga.
- 90 Commanding General, 37th Infantry Division, 37th Infantry Division, Ft. Benning, Ga.
- 91 Commanding General, 38th Infantry Division, 38th Infantry Division, Ft. Benning, Ga.
- 92 Commanding General, 39th Infantry Division, 39th Infantry Division, Ft. Benning, Ga.
- 93 Commanding General, 40th Infantry Division, 40th Infantry Division, Ft. Benning, Ga.
- 94 Commanding General, 41st Infantry Division, 41st Infantry Division, Ft. Benning, Ga.
- 95 Commanding General, 42nd Infantry Division, 42nd Infantry Division, Ft. Benning, Ga.
- 96 Commanding General, 43rd Infantry Division, 43rd Infantry Division, Ft. Benning, Ga.
- 97 Commanding General, 44th Infantry Division, 44th Infantry Division, Ft. Benning, Ga.
- 98 Commanding General, 45th Infantry Division, 45th Infantry Division, Ft. Benning, Ga.
- 99 Commanding General, 46th Infantry Division, 46th Infantry Division, Ft. Benning, Ga.
- 100 Commanding General, 47th Infantry Division, 47th Infantry Division, Ft. Benning, Ga.

### NAVY ACTIVITIES

- 68-70 Chief of Naval Operations, D/N, Washington 25, D.C. ATTN: OP-6
- 71 Chief of Naval Operations, D/N, Washington 25, D.C. ATTN: OP-6
- 72 Director of Naval Intelligence, D/N, Washington 25, D.C. ATTN: OP-907
- 73 Chief, Bureau of Medicine and Surgery, D/N, Washington 25, D.C. ATTN: Special Weapons Defense Div.
- 74 Chief, Bureau of Ordnance, D/N, Washington 25, D.C.
- 75-76 Chief of Naval Personnel, D/N, Washington 25, D.C.
- 77 Chief, Bureau of Ships, D/N, Washington 25, D.C. ATTN: Code 348
- 78 Chief, Bureau of Yards and Docks, D/N, Washington 25, D.C. ATTN: D-240
- 79 Chief, Bureau of Supplies and Accounts, D/N, Washington 25, D.C.
- 80-82 Chief, Bureau of Aeronautics, D/N, Washington 25, D.C.
- 83 Commander-in-Chief, U.S. Pacific Fleet, Fleet Post Office, San Francisco, Calif.
- 84 Commander-in-Chief, U.S. Atlantic Fleet, U.S. Naval Base, Norfolk 13, Va.
- 85 Commandant, U.S. Marine Corps, Washington 25, D.C. ATTN: Code AG3
- 86 President, U.S. Naval War College, Newport, R.I.
- 87 Superintendent, U.S. Naval Postgraduate School, Monterey, Calif.
- 88 Commanding Officer, U.S. Naval School Command, U.S. Naval Station, Treasure Island, San Francisco, Calif.
- 89 Commanding Officer, U.S. Naval Training Center, Naval Base, Norfolk 11, Va. ATTN: Special Weapons School

UNCLASSIFIED

UNCLASSIFIED

- 91 Commanding Officer, Fleet Training Center, Naval Station, San Diego, Calif. ATTN: HQ/ASST
- 92 Commanding Officer, Naval Air Station Training Center, Naval Base, Philadelphia 15, Pa. ATTN: ADM/Defense Group
- 93 Commanding Officer, U.S. Naval Air Station, Naval Air Station, Army Chemical Training Center, Ft. Belvoir, Ala.
- 94 Commander, Naval Ordnance Laboratory, Silver Spring, Md. ATTN: 7
- 95 Commander, Naval Ordnance Test Station, Inverness, Calif. ATTN: 7
- 96 Officer-in-Charge, U.S. Naval Civil Engineering Research and Development Lab., Naval Construction Center, Naval Center, Port Hueneme, Calif. ATTN: 7
- 97 Commanding Officer, Naval Medical Research and Development Command, Naval Medical Center, Bethesda 14, Md.
- 98 Director, Naval Research Laboratory, Washington 25, D.C. ATTN: MRD/Experimental
- 99 Director, Naval Ordnance Laboratory, New York Naval Shipyard, Brooklyn, N.Y.
- 100 Commanding Officer and Director, Naval Electronics Laboratory, San Diego 33, Calif. ATTN: 7
- 101-104 Chief of Staff, Naval Industrial Defense Laboratory, San Antonio 20, Calif. ATTN: 7
- 105 Commanding Officer and Director, David W. Taylor Model Basin, Washington 25, D.C. ATTN: Library
- 106 Commander, U.S. Naval Air Development Center, Jacksonville, Fla.
- 107 Commanding Officer, Technical Support Office, Case 1304, The Armory and Armory, Brooklyn, N.Y.
- 108 Commandant, U.S. Coast Guard, 1301 E. 9th St., San Francisco 21, D.C. ATTN: Capt. J. R. Stewart

AIR FORCE ACTIVITIES

- 109 Asst. for Atomic Energy, Headquarters, USAF, Washington 25, D.C. ATTN: DAF/DO
- 110 Director of Operations, Headquarters, USAF, Washington 25, D.C. ATTN: Operations Analysis
- 111 Director of Plans, Headquarters, USAF, Washington 25, D.C. ATTN: War Plans Div.
- 112 Director of Research and Development, Headquarters, USAF, Washington 25, D.C. ATTN: Combat Concepts Div.
- 113-114 Director of Intelligence, Headquarters, USAF, Washington 25, D.C. ATTN: AFM-Int
- 115 The Surgeon General, Headquarters, USAF, Washington 25, D.C. ATTN: No. 100, Army Med. Div.
- 116 Deputy Chief of Staff, Intelligence, Headquarters, USAF, Air Force Europe, APO 963, New York, N.Y. ATTN: Directorate of Air Targets
- 117 Commander, AFMTC Performance Technical Division (Management), APO 963, New York, N.Y.
- 118 Commander, Far East Air Service, APO 963, San Francisco, Calif.
- 119 Commander-in-Chief, Strategic Air Command, Offutt Air Force Base, Omaha, Nebraska. ATTN: Special Weapons Branch, Inspector Div., Inspector General
- 120 Commander, Tactical Air Command, Langley AFB, Va. ATTN: Documents Security Branch
- 121 Commander, Air Defense Command, Fort APD, Colo.
- 122-123 Commander, Wright Air Development Center, Wright Patterson AFB, Dayton, O. ATTN: AFMTC, Joint Effects Research
- 124 Commander, Air Training Command, Scott AFB, Belleville, Ill. ATTN: DM/AF/STP
- 125 Assistant Chief of Staff, Installations, Headquarters, USAF, Washington 25, D.C. ATTN: AFMTC
- 126 Commander, Air Research and Development Command, 10 Sam 1124, Baltimore, Md. ATTN: MRD
- 127 Commander, Air Proving Ground Command, Eglin AFB, Fla. ATTN: Adm./Tech. Support Branch

- 128 Director, Air Research and Development Command, 10 Sam 1124, Baltimore, Md. ATTN: MRD
- 129 Director, Air Research and Development Command, 10 Sam 1124, Baltimore, Md. ATTN: MRD
- 130 Director, Air Research and Development Command, 10 Sam 1124, Baltimore, Md. ATTN: MRD
- 131 Director, Air Research and Development Command, 10 Sam 1124, Baltimore, Md. ATTN: MRD
- 132 Director, Air Research and Development Command, 10 Sam 1124, Baltimore, Md. ATTN: MRD
- 133 Director, Air Research and Development Command, 10 Sam 1124, Baltimore, Md. ATTN: MRD
- 134 Director, Air Research and Development Command, 10 Sam 1124, Baltimore, Md. ATTN: MRD
- 135 Director, Air Research and Development Command, 10 Sam 1124, Baltimore, Md. ATTN: MRD
- 136 Director, Air Research and Development Command, 10 Sam 1124, Baltimore, Md. ATTN: MRD
- 137 Director, Air Research and Development Command, 10 Sam 1124, Baltimore, Md. ATTN: MRD
- 138 Director, Air Research and Development Command, 10 Sam 1124, Baltimore, Md. ATTN: MRD
- 139 Director, Air Research and Development Command, 10 Sam 1124, Baltimore, Md. ATTN: MRD
- 140 Director, Air Research and Development Command, 10 Sam 1124, Baltimore, Md. ATTN: MRD
- 141 Director, Air Research and Development Command, 10 Sam 1124, Baltimore, Md. ATTN: MRD
- 142 Director, Air Research and Development Command, 10 Sam 1124, Baltimore, Md. ATTN: MRD
- 143 Director, Air Research and Development Command, 10 Sam 1124, Baltimore, Md. ATTN: MRD
- 144 Director, Air Research and Development Command, 10 Sam 1124, Baltimore, Md. ATTN: MRD
- 145 Director, Air Research and Development Command, 10 Sam 1124, Baltimore, Md. ATTN: MRD
- 146 Director, Air Research and Development Command, 10 Sam 1124, Baltimore, Md. ATTN: MRD
- 147 Director, Air Research and Development Command, 10 Sam 1124, Baltimore, Md. ATTN: MRD
- 148 Director, Air Research and Development Command, 10 Sam 1124, Baltimore, Md. ATTN: MRD
- 149 Director, Air Research and Development Command, 10 Sam 1124, Baltimore, Md. ATTN: MRD
- 150 Director, Air Research and Development Command, 10 Sam 1124, Baltimore, Md. ATTN: MRD

- 151 Asst. Secretary for Operations, Headquarters, USAF, Washington 25, D.C. ATTN: DAF/DO
- 152 Director of Operations, Headquarters, USAF, Washington 25, D.C. ATTN: Operations Analysis
- 153 Director of Plans, Headquarters, USAF, Washington 25, D.C. ATTN: War Plans Div.
- 154 Director of Research and Development, Headquarters, USAF, Washington 25, D.C. ATTN: Combat Concepts Div.
- 155 Director of Intelligence, Headquarters, USAF, Washington 25, D.C. ATTN: AFM-Int
- 156 The Surgeon General, Headquarters, USAF, Washington 25, D.C. ATTN: No. 100, Army Med. Div.
- 157 Deputy Chief of Staff, Intelligence, Headquarters, USAF, Air Force Europe, APO 963, New York, N.Y. ATTN: Directorate of Air Targets
- 158 Commander, AFMTC Performance Technical Division (Management), APO 963, New York, N.Y.
- 159 Commander, Far East Air Service, APO 963, San Francisco, Calif.
- 160 Commander-in-Chief, Strategic Air Command, Offutt Air Force Base, Omaha, Nebraska. ATTN: Special Weapons Branch, Inspector Div., Inspector General
- 161 Commander, Tactical Air Command, Langley AFB, Va. ATTN: Documents Security Branch
- 162 Commander, Air Defense Command, Fort APD, Colo.
- 163-164 Commander, Wright Air Development Center, Wright Patterson AFB, Dayton, O. ATTN: AFMTC, Joint Effects Research
- 165 Commander, Air Training Command, Scott AFB, Belleville, Ill. ATTN: DM/AF/STP
- 166 Assistant Chief of Staff, Installations, Headquarters, USAF, Washington 25, D.C. ATTN: AFMTC
- 167 Commander, Air Research and Development Command, 10 Sam 1124, Baltimore, Md. ATTN: MRD
- 168 Commander, Air Proving Ground Command, Eglin AFB, Fla. ATTN: Adm./Tech. Support Branch

- 169 Director, Air Research and Development Command, 10 Sam 1124, Baltimore, Md. ATTN: MRD
- 170 Director, Air Research and Development Command, 10 Sam 1124, Baltimore, Md. ATTN: MRD
- 171 Director, Air Research and Development Command, 10 Sam 1124, Baltimore, Md. ATTN: MRD
- 172 Director, Air Research and Development Command, 10 Sam 1124, Baltimore, Md. ATTN: MRD
- 173 Director, Air Research and Development Command, 10 Sam 1124, Baltimore, Md. ATTN: MRD
- 174 Director, Air Research and Development Command, 10 Sam 1124, Baltimore, Md. ATTN: MRD
- 175 Director, Air Research and Development Command, 10 Sam 1124, Baltimore, Md. ATTN: MRD
- 176 Director, Air Research and Development Command, 10 Sam 1124, Baltimore, Md. ATTN: MRD
- 177 Director, Air Research and Development Command, 10 Sam 1124, Baltimore, Md. ATTN: MRD
- 178 Director, Air Research and Development Command, 10 Sam 1124, Baltimore, Md. ATTN: MRD
- 179 Director, Air Research and Development Command, 10 Sam 1124, Baltimore, Md. ATTN: MRD
- 180 Director, Air Research and Development Command, 10 Sam 1124, Baltimore, Md. ATTN: MRD

UNCLASSIFIED

Unclassified

THIS REPORT HAS BEEN DELIMITED  
AND CLEARED FOR PUBLIC RELEASE  
UNDER DOD DIRECTIVE 5200.20 AND  
NO RESTRICTIONS ARE IMPOSED UPON  
ITS USE AND DISCLOSURE.

DISTRIBUTION STATEMENT A

APPROVED FOR PUBLIC RELEASE,  
DISTRIBUTION UNLIMITED.